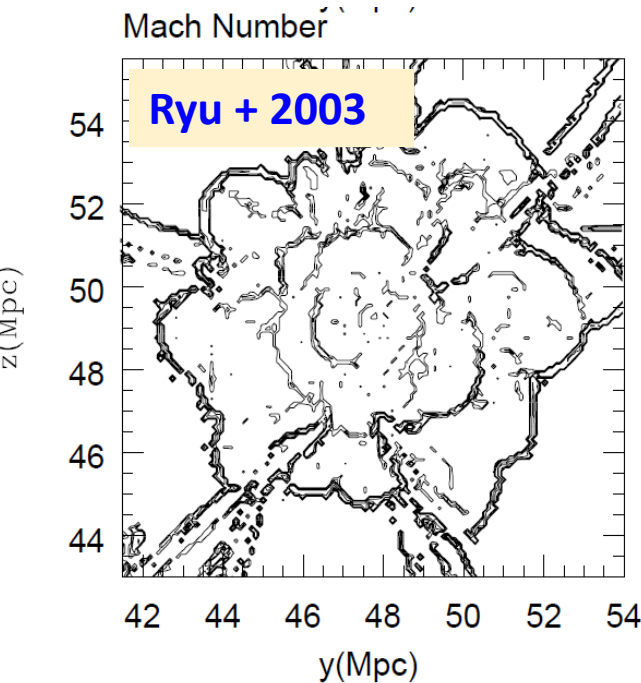


Particle Acceleration at Structure Formation Shocks

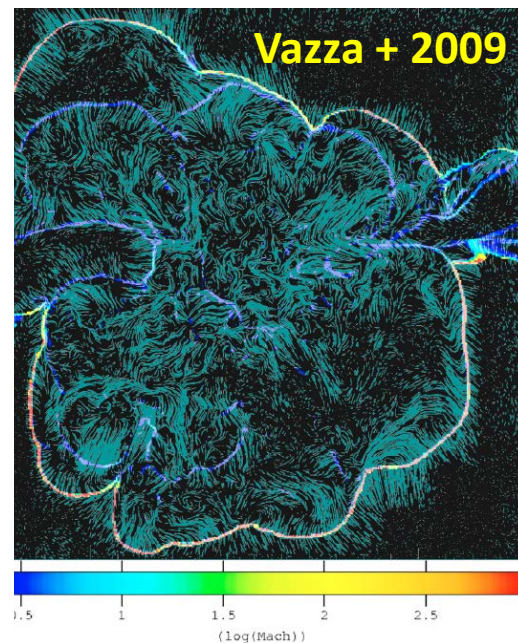
Hyesung Kang (Pusan National University)

Dongsu Ryu (UNIST, Korea)

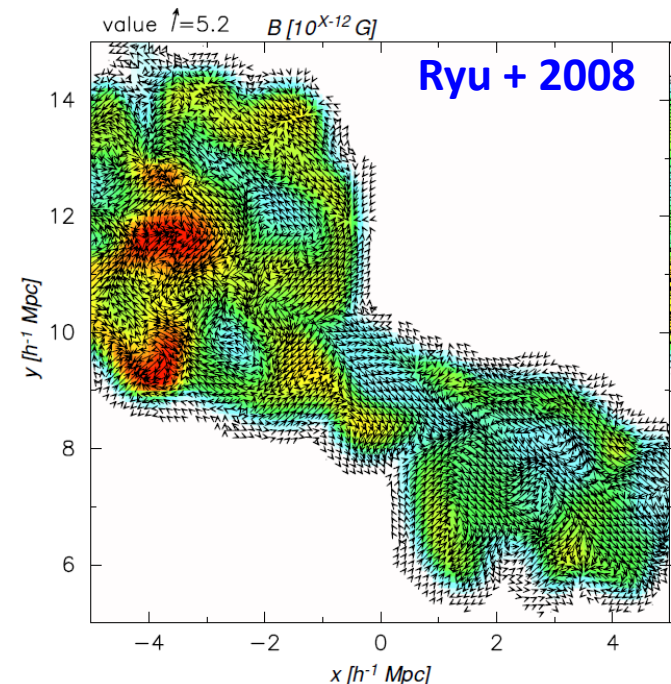
T. W. Jones (Univ. of Minnesota)



Shocks

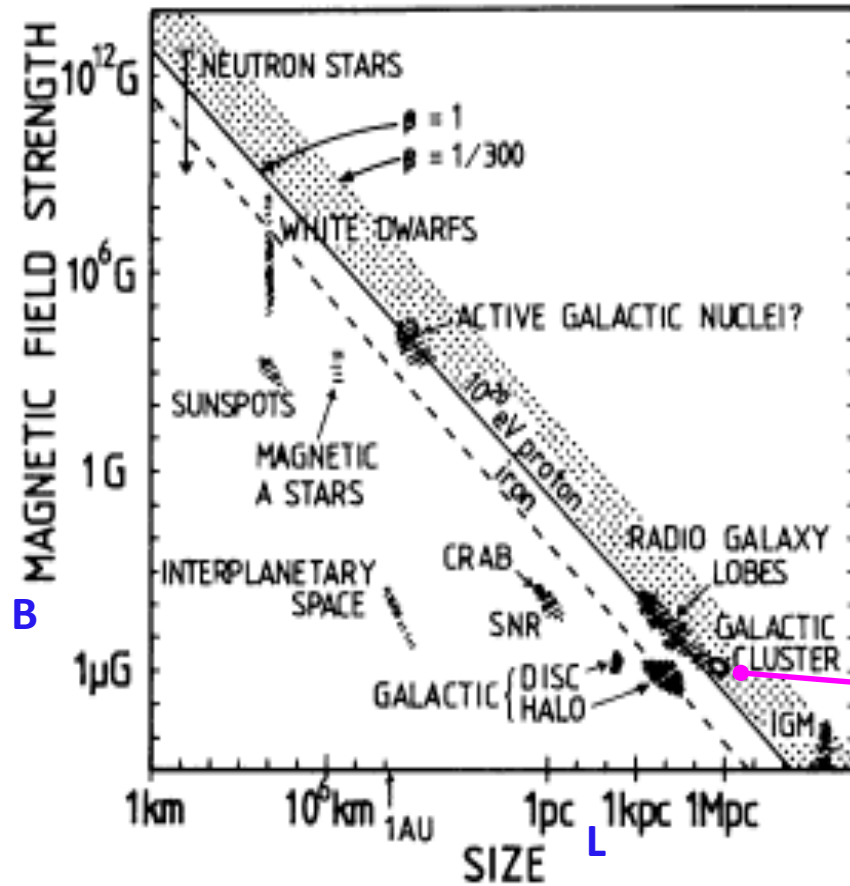


Turbulence



Magnetic Fields

Size limited E_{\max} for acceleration sites: Hillas Diagram



THE ORIGIN OF ULTRA-HIGH-ENERGY COSMIC RAYS

A. M. Hillas

ARAA 1984

$$B_{\mu\text{G}} L_{\text{pc}} > \frac{E_{15}}{Z\beta_a}$$

$$\beta_a = V_a / c$$

galaxy clusters:

$$B \sim 1\mu\text{G}, \quad L \sim 100\text{kpc}$$

$$\beta \sim 0.01, \quad E_{\max} \sim 10^{18} \text{ eV}$$

Figure 1 Size and magnetic field strength of possible sites of particle acceleration. Objects below the diagonal line cannot accelerate protons to 10^{20} eV.

Bow shocks of galaxies in ICM, rather than structure formation shocks such as accretion shocks.

THE ORIGIN OF COSMIC RAYS ABOVE $10^{18.5}$ eV

COLIN A. NORMAN,^{1,2,3} DONALD B. MELROSE,³ AND ABRAHAM ACHTERBERG⁴

Received 1994 August 8; accepted 1995 June 1

MAXIMUM ENERGIES

Norman et al. 1995

Source	E_m	D_{\max}	$\langle n \rangle D_{\max}^3$
AGN	10^{16} eV	~ 3 Gpc	10^5
Jets	10^{20} eV	200 Mpc	~ 10
Cocoons	5×10^{19} eV	500 Mpc	~ 100
Clusters	10^{19} eV	1 Gpc	$\sim 10^4$
Superclusters	5×10^{19} eV	500 Mpc	~ 100

Cosmic shocks, formed as structure develops in the gravitational collapse of primordial perturbations as seen in the standard cosmological models such as in pancake-like structures, and in the collisions of hierarchical merging subunits, are also possible sites for the UHECR acceleration up to $10^{19.5}$ eV, provided there is a primordial field of $\gtrsim 10^{-9}$ G or if micro-gauss fields can be self-generated in shocks.

CLUSTER ACCRETION SHOCKS AS POSSIBLE ACCELERATION SITES FOR ULTRA-HIGH-ENERGY PROTONS BELOW THE GREISEN CUTOFF

HYESUNG KANG

Department of Earth Sciences, Pusan National University, Pusan 609-735, Korea; kang@astrophys.es.pusan.ac.kr

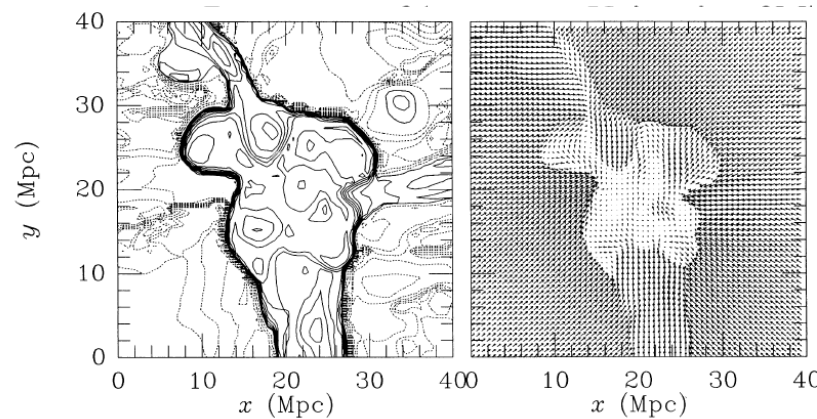
DONGSU RYU

Department of Astronomy & Space Science, Chungnam National University, Daejeon 305-764, Korea; ryu@sirius.chungnam.ac.kr

AND

Kang, Ryu & Jones 1996

T. W. JONES

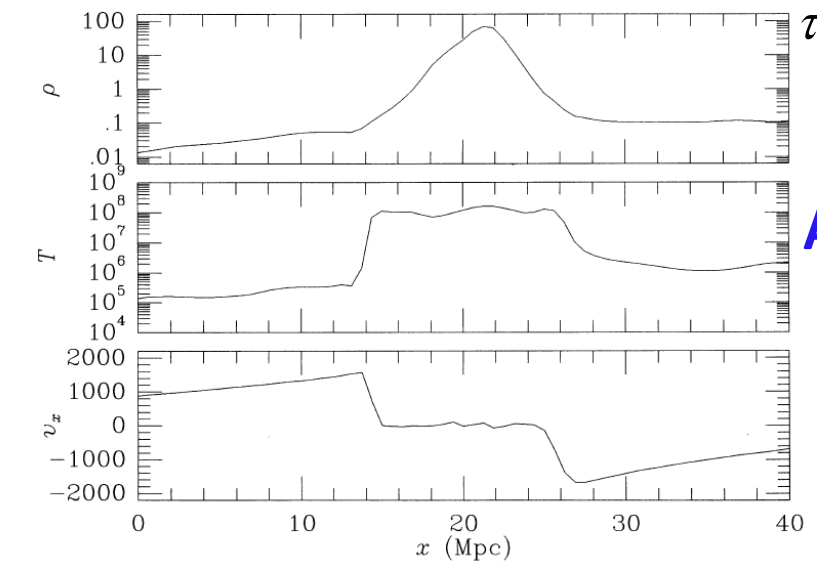


$$\text{for } \kappa_{Bohm}(\rho) = \kappa^* \cdot \rho \cdot \left(\frac{\rho_0}{\rho}\right)$$

$$\tau_{acc}(\rho) \approx \frac{3}{u_1 - u_2} \left(\frac{\kappa_1(\rho)}{u_1} + \frac{\kappa_2(\rho)}{u_2} \right) : \text{mean accel. time for DSA}$$

$$\tau_{pp} \sim 5 \times 10^9 \text{ years: photo-pair loss time at } 10^{19} \text{ eV}$$

$$\tau_{acc} \sim \tau_{pp} \Rightarrow p_{max} \simeq \frac{E_{max}}{m_p c^2} \simeq 1.4 \times 10^{10} \left(\frac{u_s}{1500 \text{ km s}^{-1}} \right)^2 B_\mu$$



Accretion shocks, proton acceleration

for $u_s = 3000 \text{ km/s}$, $B = 1 \mu\text{G}$

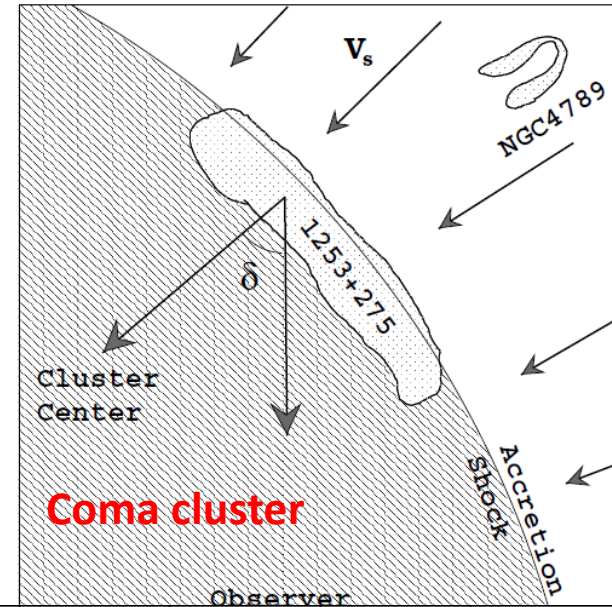
$$E_{max} \sim 6 \times 10^{19} \text{ eV}$$

Cluster radio relics as a tracer of shock waves of the large-scale structure formation

Ensslin et al. 1998

Torsten A. Enßlin¹, Peter L. Biermann¹, Ulrich Klein², and Sven Kohle²

Observational evidence for structure formation shocks =radio relics : diffuse synchrotron emission from re-energized fossil electrons by accretion shock in the cluster outskirts.

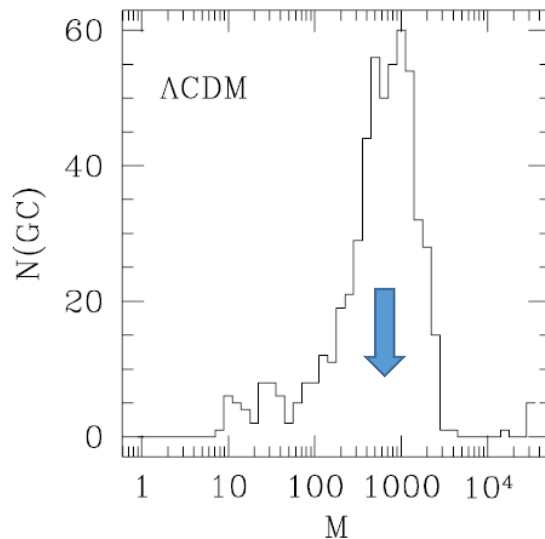
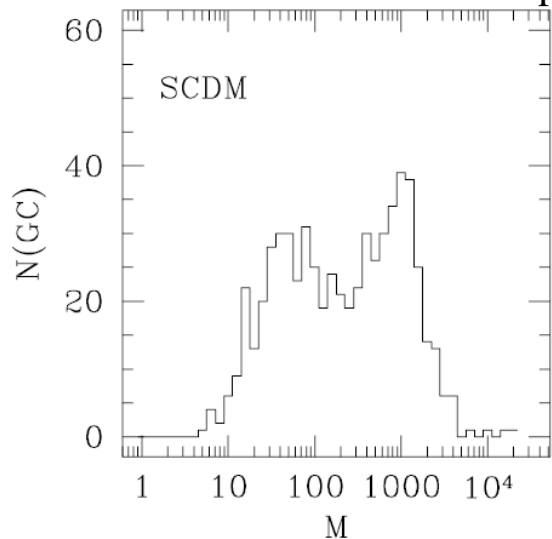


Cluster Relic		References	A85 0038-096	A786 0917+75	A1367 1140+203	Coma 1253+275	A2255 1712+64	A2256 1706+78	A3667 2006-56	S753 1401-33
z		fovfffn	0.0559	0.125	0.0216	0.0233	0.0824	0.0824	0.0566	0.0142
kT_{obs}	keV	e-dbdrf	6.2	—	3.7	8.2	7.3	7.3	6.3	2.5 ⁽⁶⁾
$n_{e,o}$	$10^{-3} \text{ cm}^{-3} h_{50}^{1/2}$	p-pbhpr-	5.5	—	0.95	3	1.8	2.5	1	—
r_{core}	kpc h_{50}^{-1}	p-pbhar-	225	—	430	400	579	352	286	—
β		e-pbhar-	0.62	—	0.52	0.75	0.74	0.76	0.54	—
$r_{\text{projected}}$	Mpc h_{50}^{-1}	soilhtmn	0.64	5	1.09	2.9	1.25	0.74	2.95	0.911
α		gojlhtun	>1.5 ⁽¹⁾	1.1	1.9	1.18	1.4	0.8 ⁽²⁾	1.1	1.4
P	%	-ol-ht-	—	54	—	27	<2	20	—	—
$B_{2,eq}$	$\mu\text{G} h_{50}^{2/7}$	gojlhtmn	<1.4	0.5	2	0.7	0.6	2.7	1.6	0.4

PROPERTIES OF COSMIC SHOCK WAVES IN LARGE-SCALE STRUCTURE FORMATION

FRANCESCO MINIATI,¹ DONGSU RYU,² HYESUNG KANG,³ T. W. JONES,¹ RENYUE CEN,⁴ AND JEREMIAH P. OSTRIKER⁴

External shocks: $r > 0.5h^{-1}\text{Mpc}$

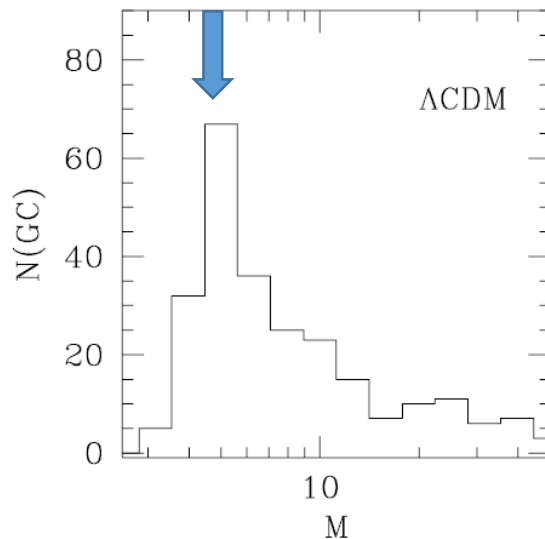
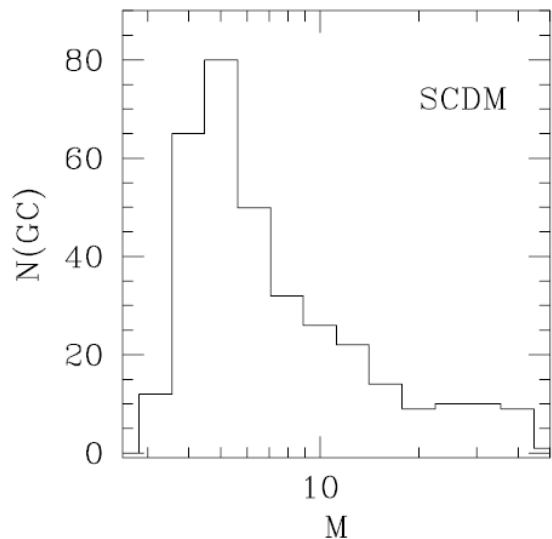


Miniati et al. 2000

External shocks = accretion shocks with high Mach numbers

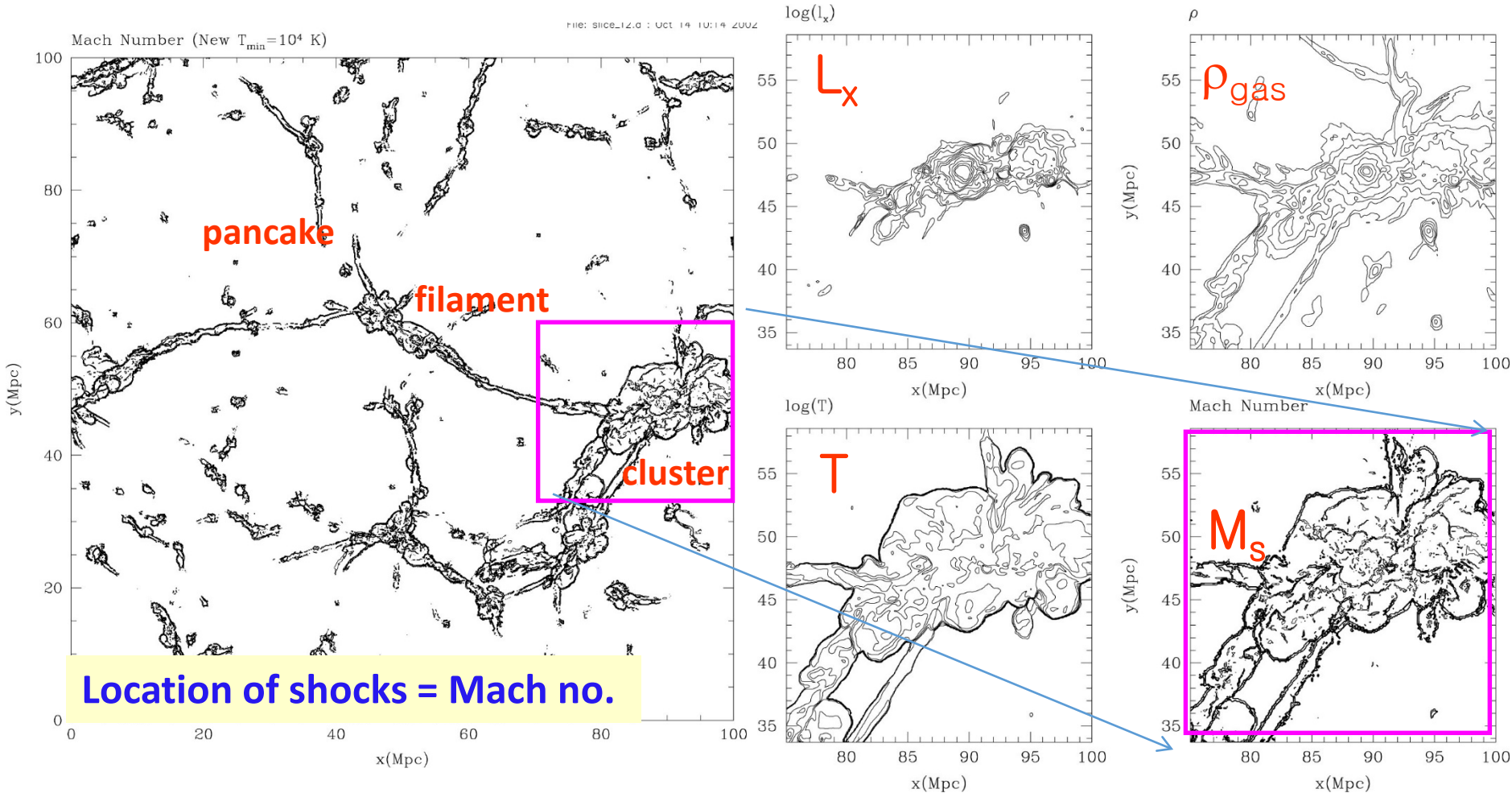
Possible acceleration sites for UHECRs

Internal shocks: $r < 0.5h^{-1}\text{Mpc}$



Internal shocks = merger shocks, flow shocks with low Mach numbers

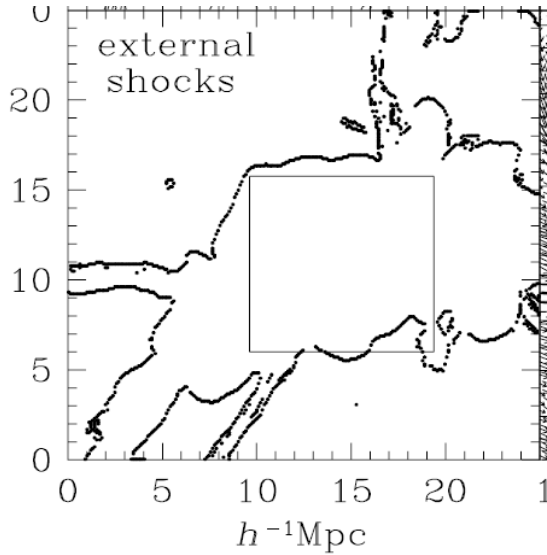
Shocks in Structure Formation Simulations



Miniati et al. 2000; Keshet et al. 2003; Ryu et al. 2003;
Pfrommer et al. 2006; Kang et al. 2007; Skillman et al. 2008;
Hoefl et al. 2008; Vazza et al. 2009; Pinzke et al. 2013;
+ many Later papers by these authors and others

Shocks in Structure Formation Simulations (Ryu et al 2003)

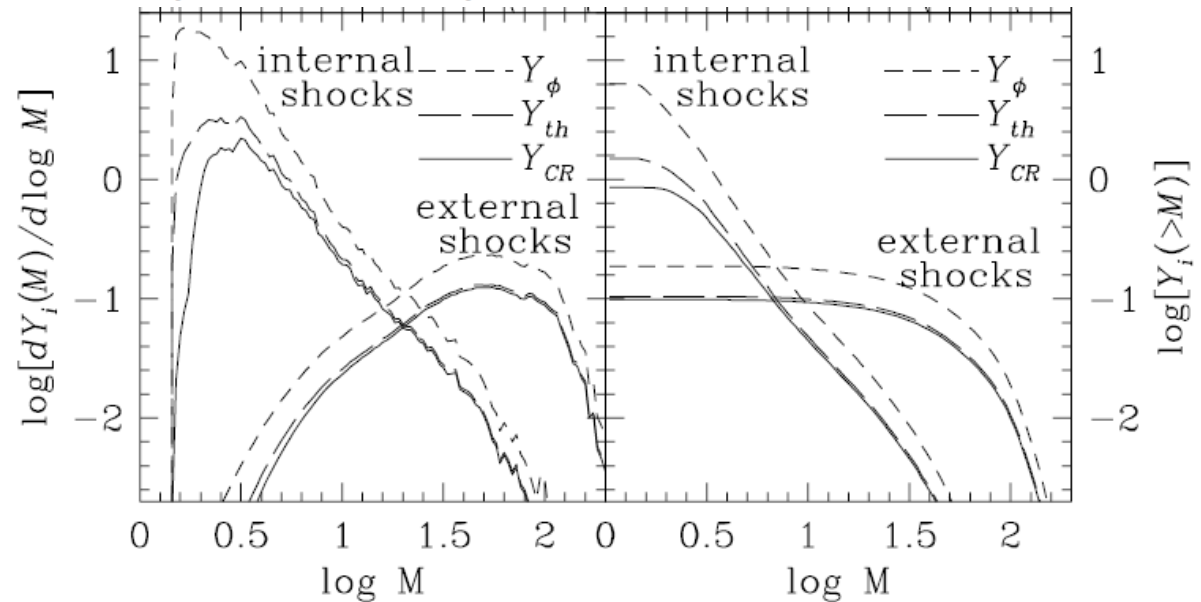
Accretion Shocks



At **Strong accretion shocks** with $V_s \sim 1000-3000$ km/s
 $M \sim 10-100$ DSA efficiency could be high as in SNRs.

Energy generation function: $Y_i(M)$

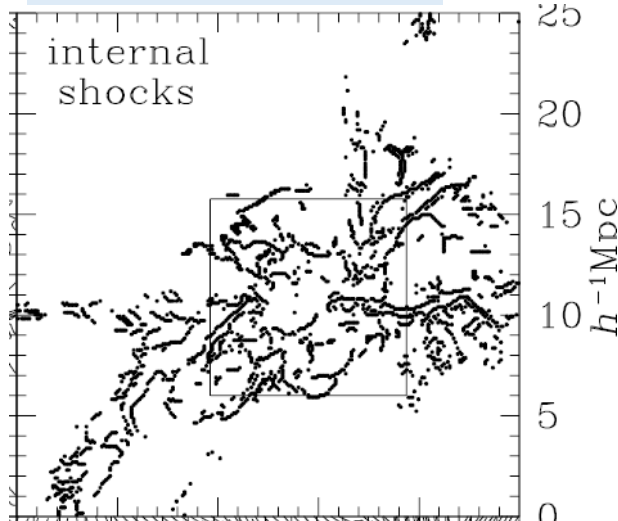
$$\frac{dY_i(M)}{d \log M} = \frac{1}{\mathcal{N}_i} \int_{z=2}^{z=0} \frac{dF_i(M, z)}{d \log M} dt \quad Y_i(> M) = \int_{\infty}^M \left[\frac{dY_i(M)}{d \log M} \right] d \log M$$



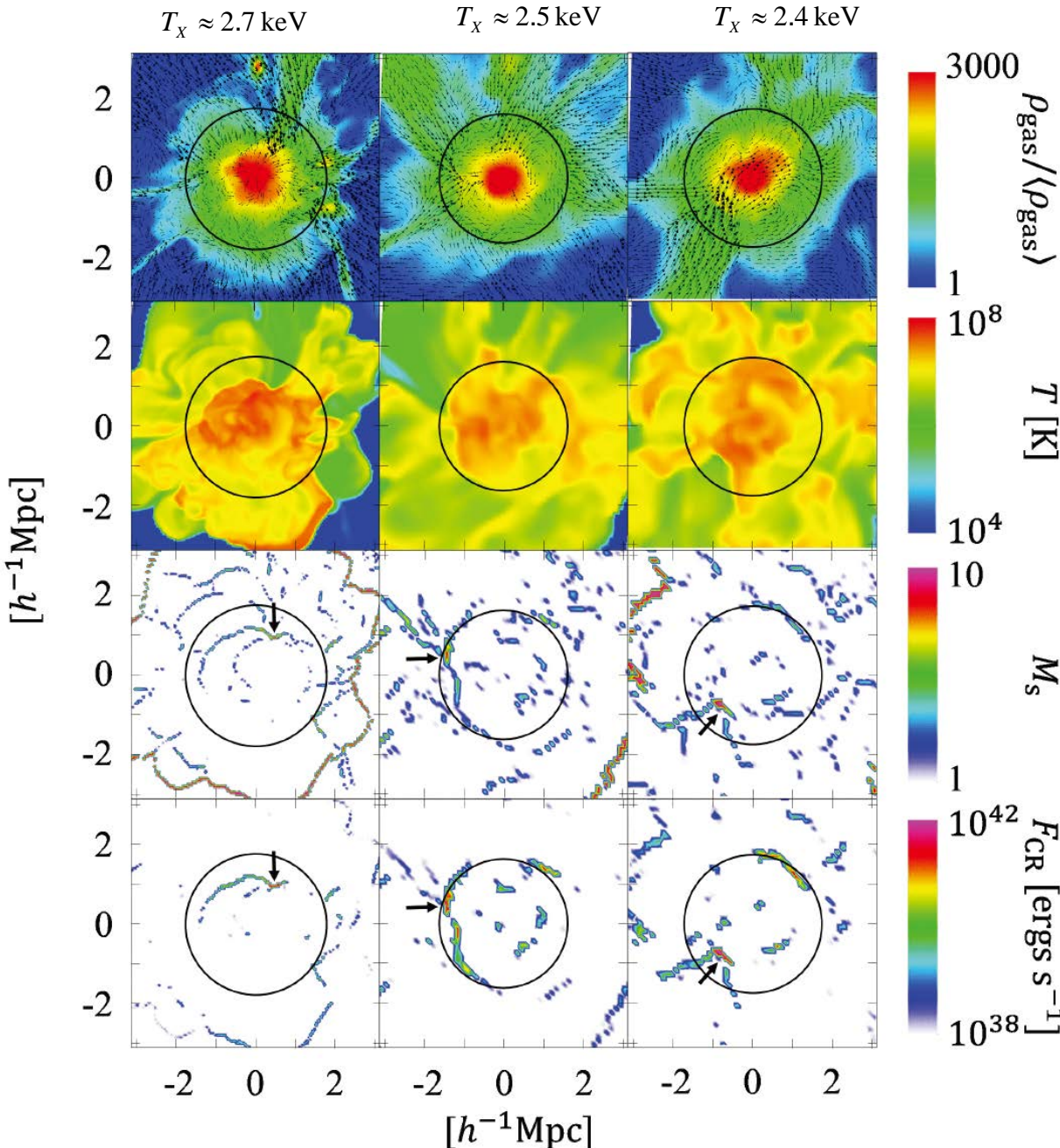
ϕ = kinetic energy, th = thermal energy, CR = cosmic ray energy

Weak internal shocks with $M < 3$ are dominant inside ICM and energetically important.

Shocks in ICM



Shock Waves in the Outskirts of simulated clusters: filament accretion



- infalls of high ρ , low T filament gas
- penetrate deep in to ICM

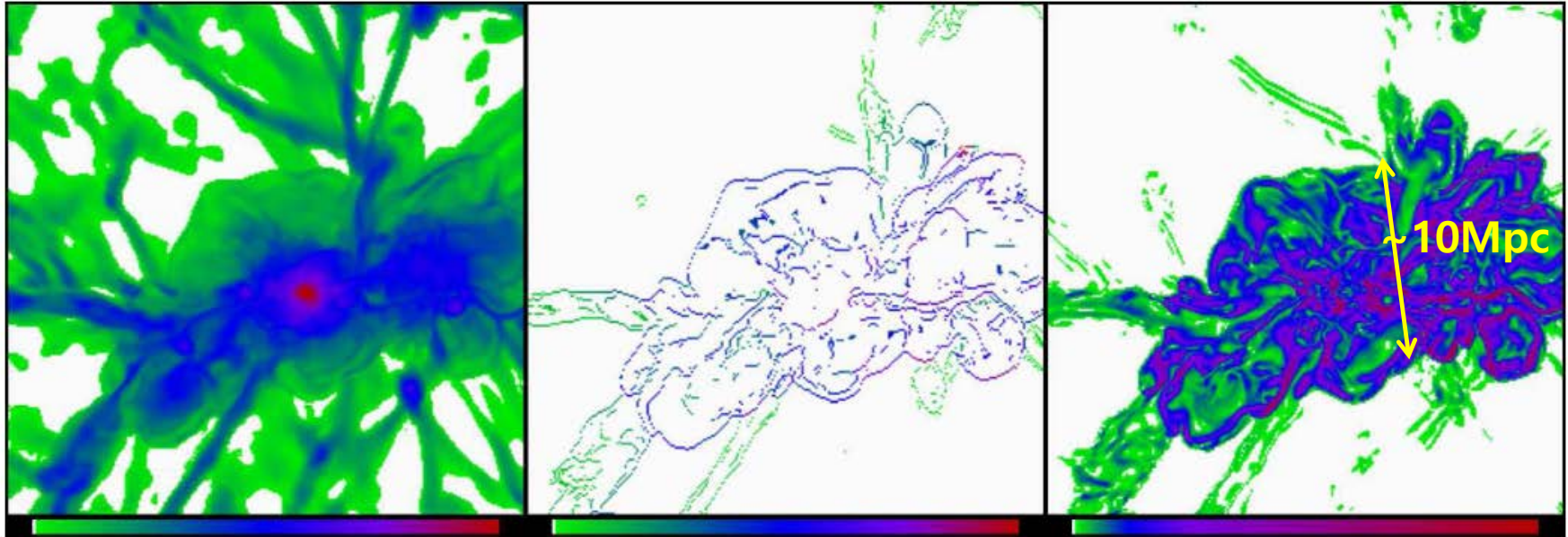
Energetic Accretion Shocks

- $3 < M_s < 10$
- Thin elongated arc-like morphology similar to radio relics.
- Mach number varies along the connected shocked zones.

$$- f_{\text{CR}} > 10^{42} \text{ erg/s}/(h^{-1}\text{Mpc})^2$$

B fields in LSS

gravitational collapse \rightarrow cosmological shocks \rightarrow vorticity & turbulence \rightarrow B field amplification via turbulence dynamo



gas density

$(25h^{-1}\text{Mpc})^2$

shock locations:

color coded with V_{shock}

vorticity

Ryu et al 2008

- Λ cold dark matter cosmology

$\Omega_{\Lambda} = 0.73$, $\Omega_{\text{DM}} = 0.23$, $\Omega_{\text{gas}} = 0.043$, $h=0.7$, $n = 1$, $\sigma_8 = 0.8$

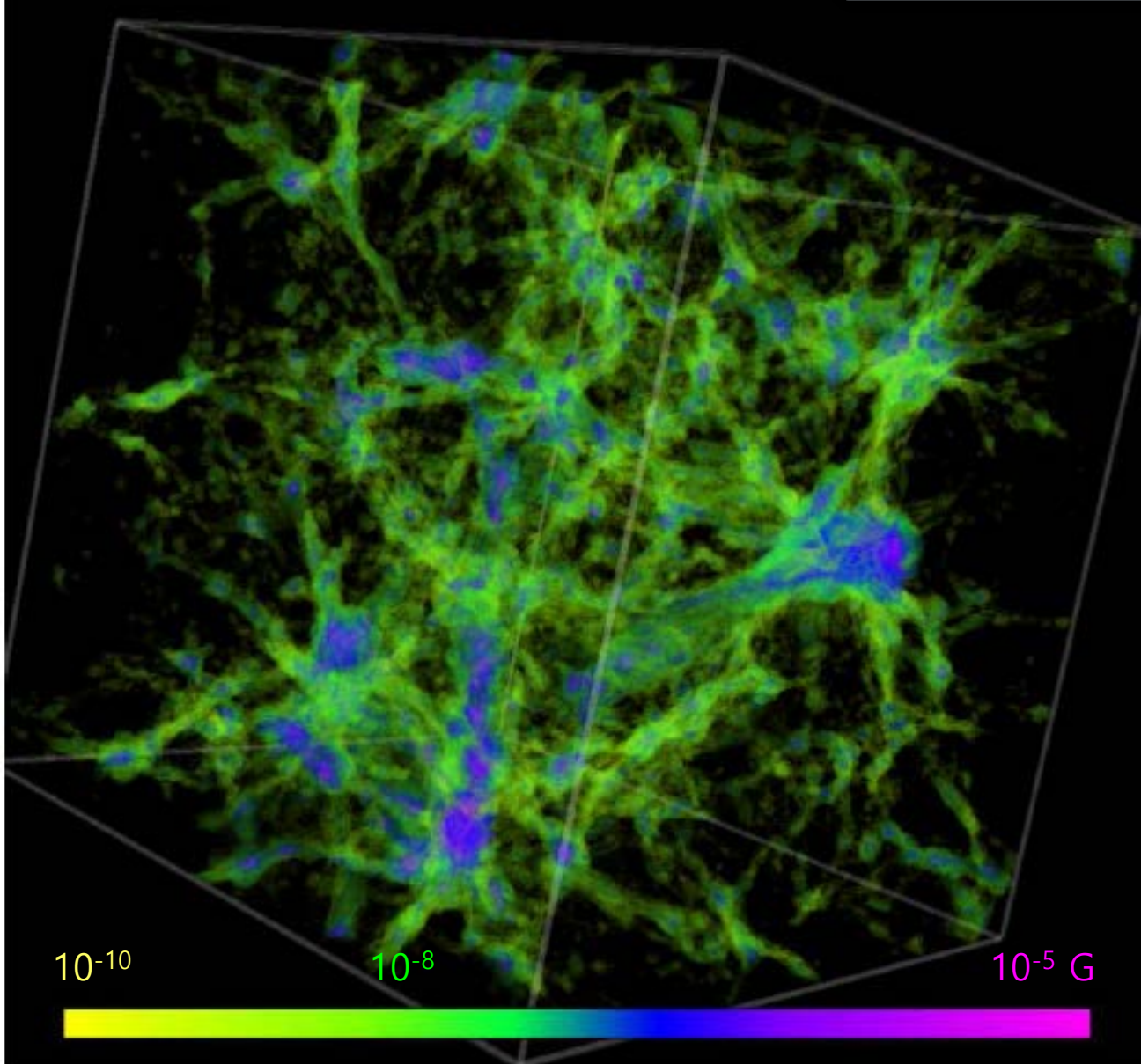
-computational box: $(143 \text{ Mpc})^3$: grid-based Eulerian TVD code: Hydrodynamic Sim

With passively evolving B field: **B=0 initially, generated at shocks**

via Biermann Battery and amplified by flow motions

Magnitude of B based on turbulence dynamo: vorticity & $E_{\text{turb}} \rightarrow E_B$

B field strength in the cosmic web



Color code:

Blue: clusters, $1\mu\text{G}$

Green: filaments, 10nG

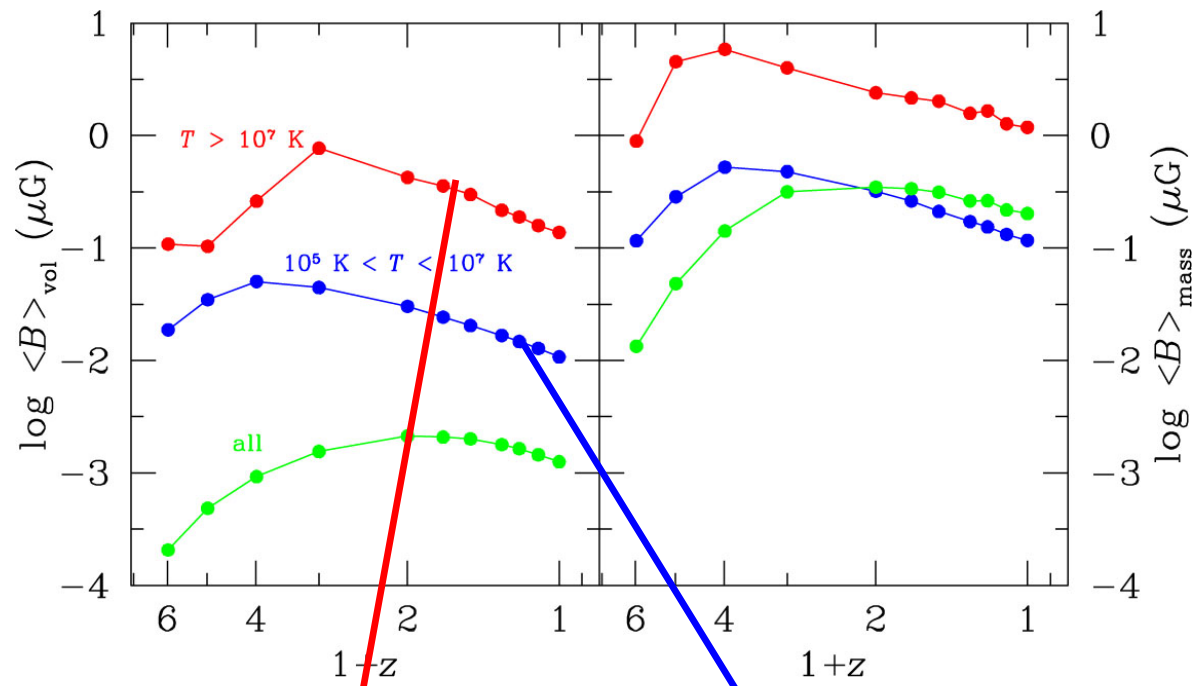
at each grid point

$$\vec{\omega} = \vec{\nabla} \times \vec{v}$$

$$E_{\text{turb}} = \frac{1}{2} \rho v_{\text{curl}}^2$$

$$\begin{aligned} \Rightarrow E_{\text{mag}} &= \phi(\omega t) \cdot E_{\text{turb}} \\ &= \frac{B^2}{8\pi} \end{aligned}$$

Ryu et al 2008



**magnetic field strength
via turbulent dynamo**

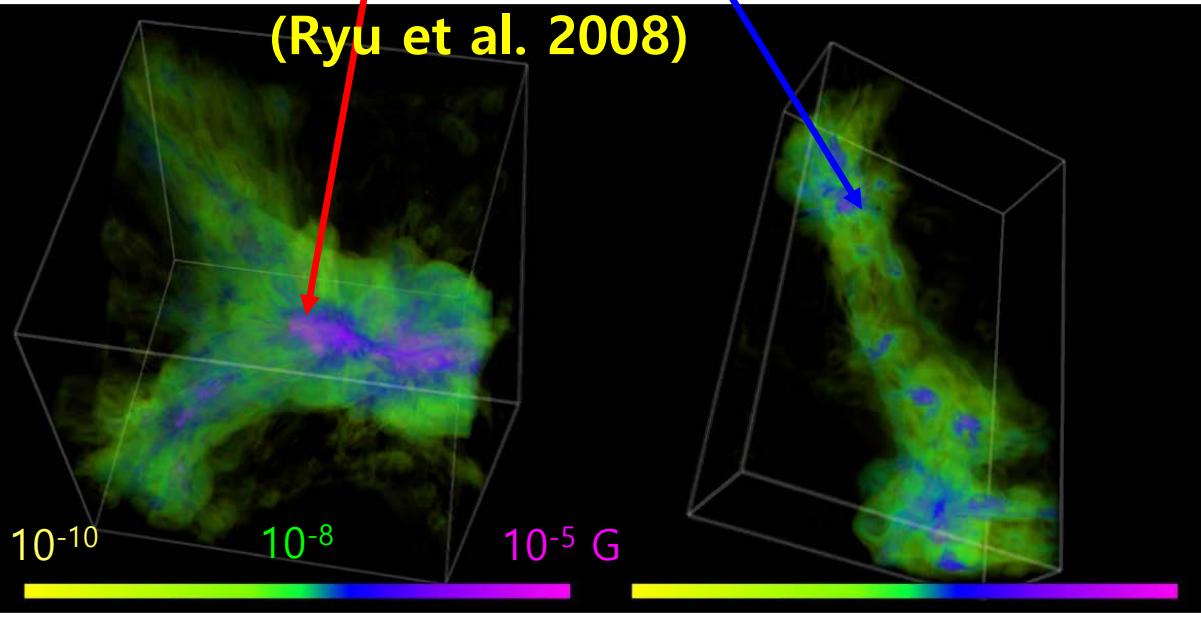
-in & around clusters :

$\langle B \rangle_{\text{vol}} \sim 0.1 \mu\text{G}$

-in filaments:

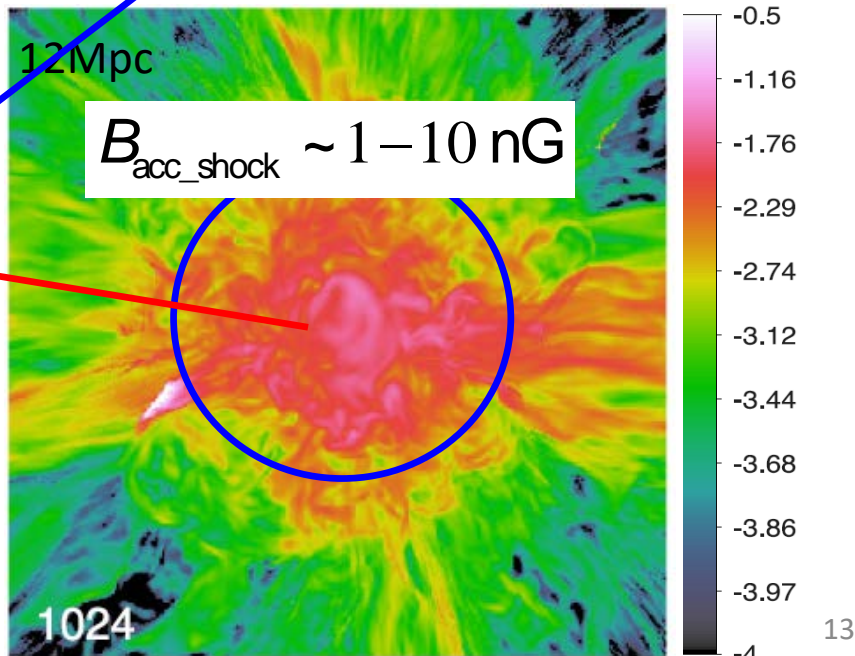
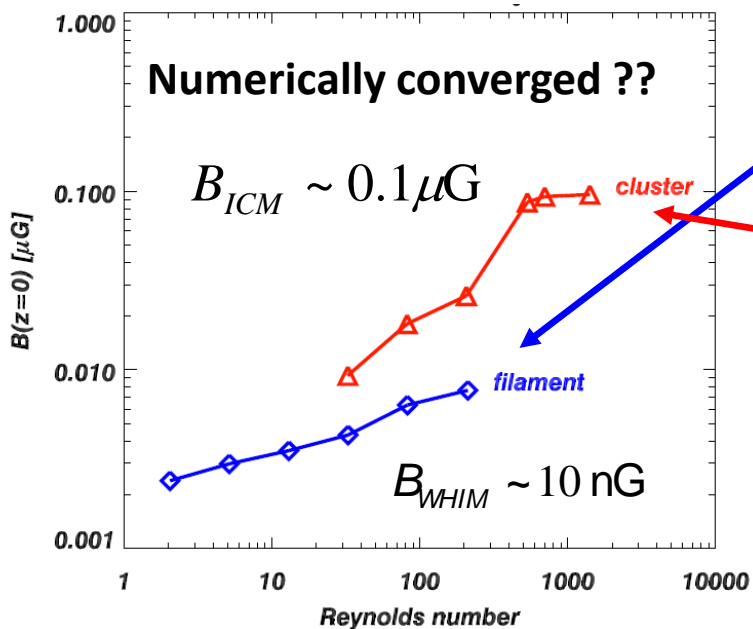
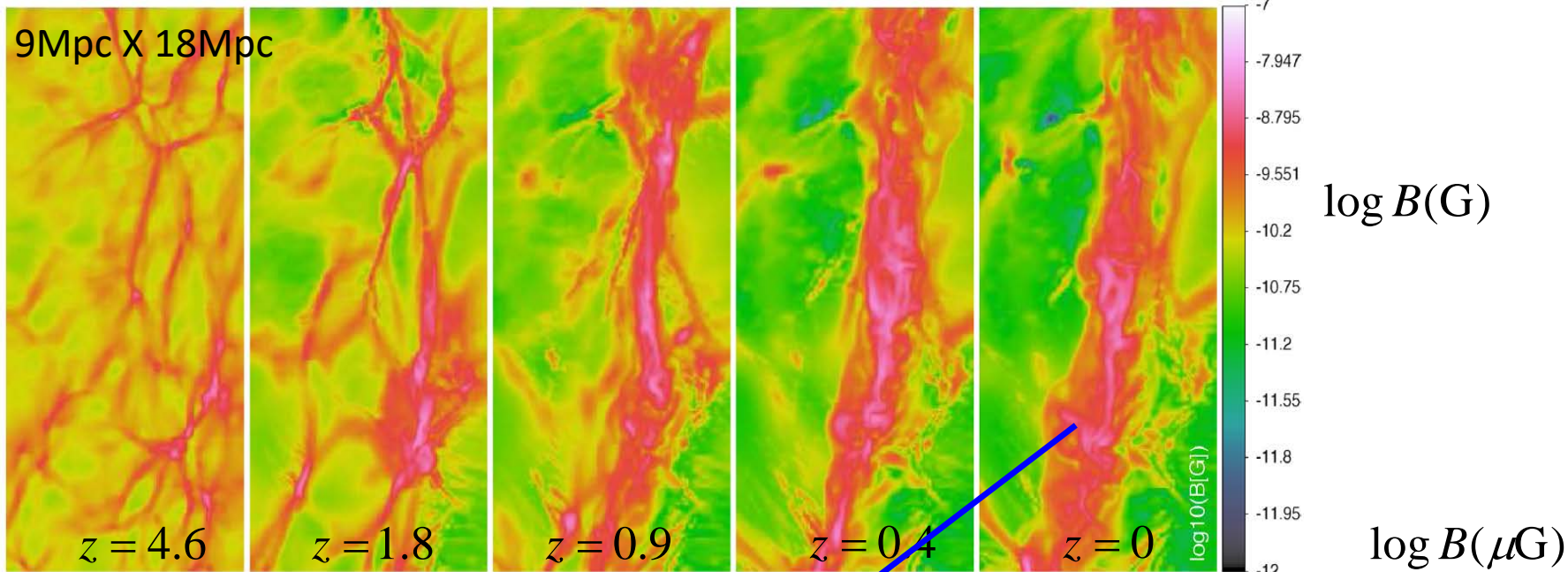
$\langle B \rangle_{\text{vol}} \sim 10 \text{ nG}$

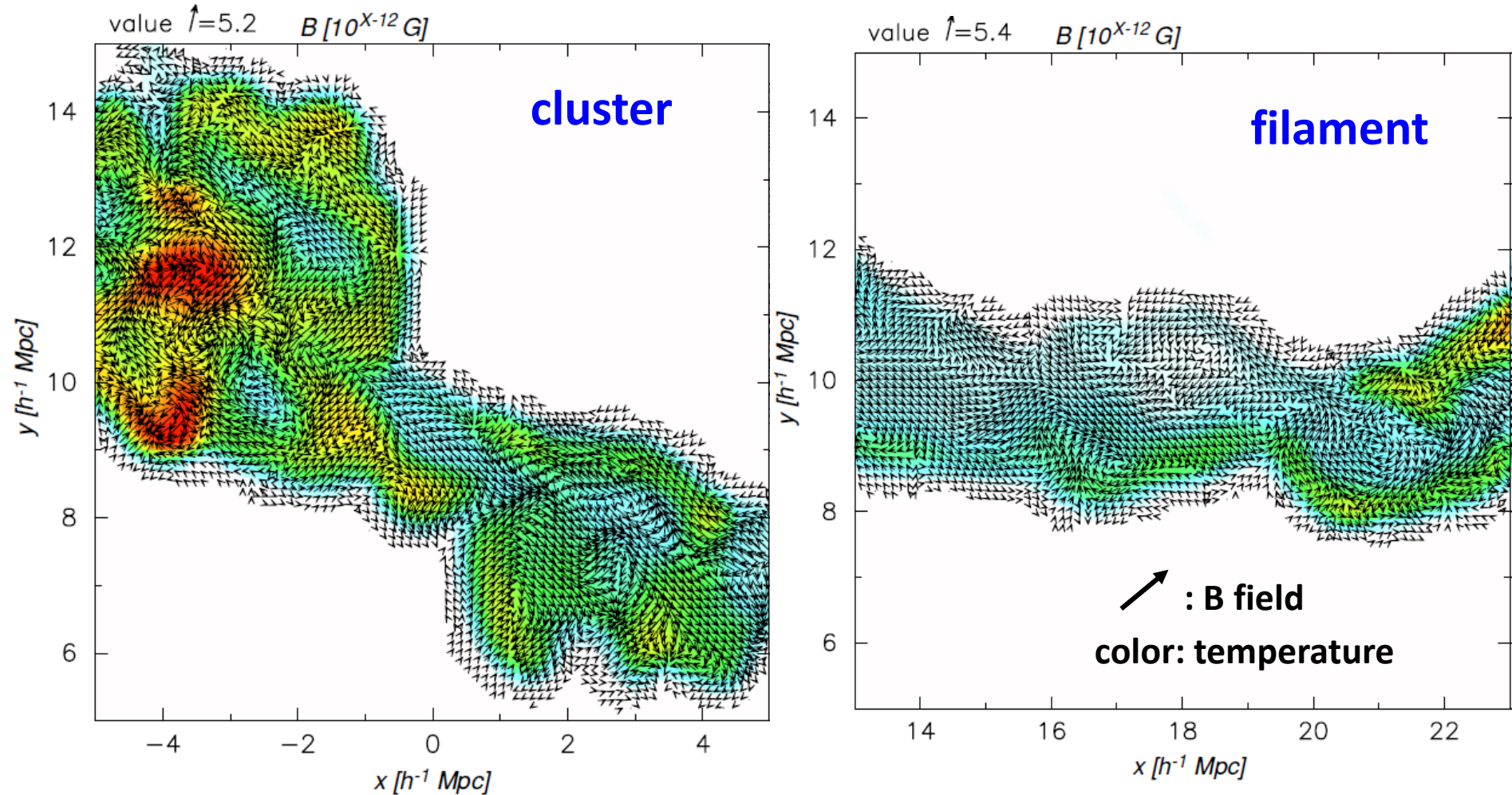
(Ryu et al. 2008)



Many studies since then:
Vazza et al 2011 - 2016
Cho 2014
Miniati 2014, 2015
Beresnyak & Miniati 2016

MHD simulations (ENZO): Vazza et al 2014 → to see small-scale turbulent dynamo (?)



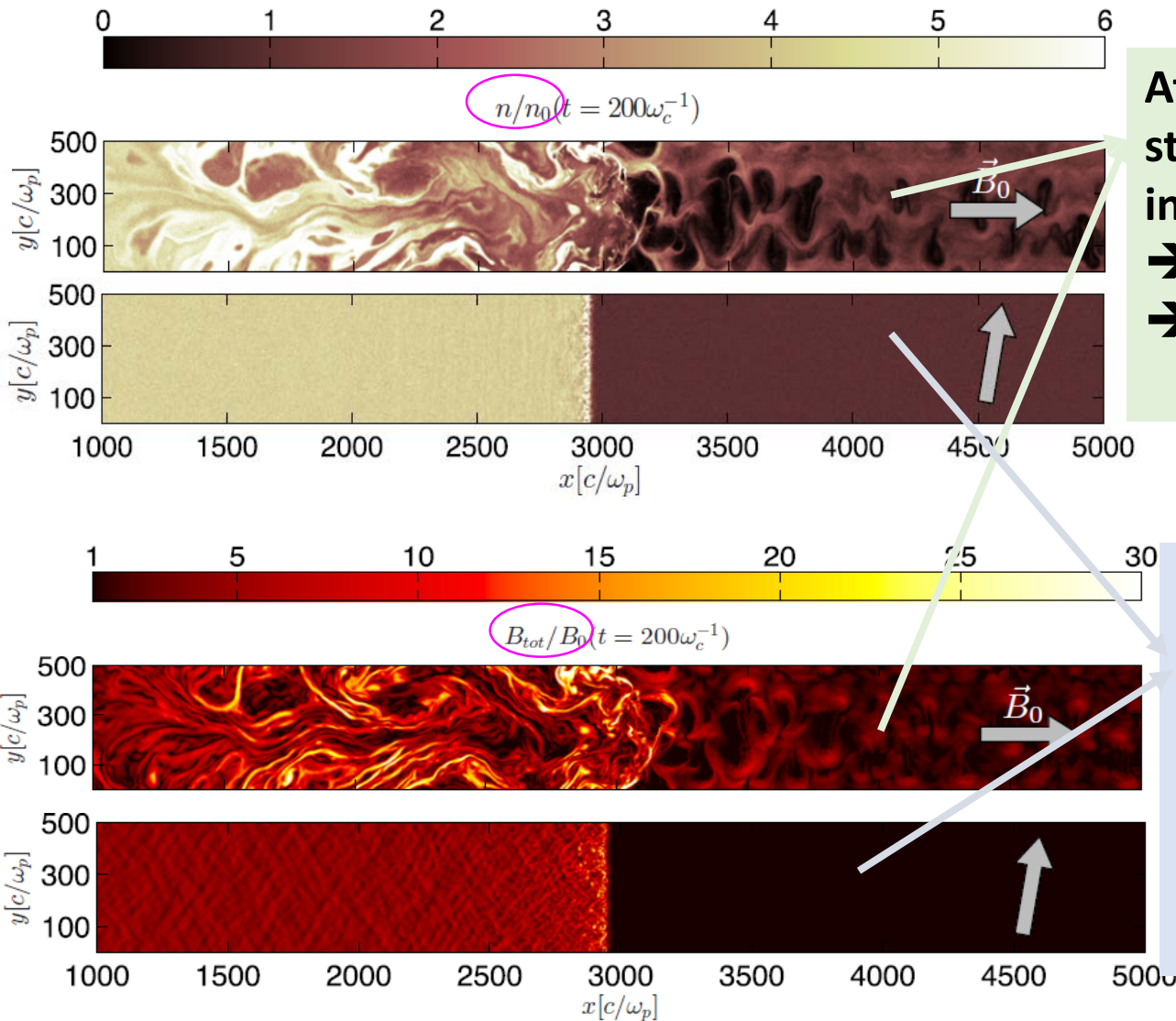


- Accretion shocks encompass the outer surface of clusters and filaments.
- Magnetic field vectors are random with coherent length of 100-130 kpc.
- PDF of obliquity angle: $P(\theta) \propto \sin \theta$ for random orientation of B
- Q-perp shocks (70%) are preferred over Q-par shocks (30%)

DSA Obliquity Dependence: 2D Hybrid Simulations (CRp)

Caprioli & Sptikovsky 2014

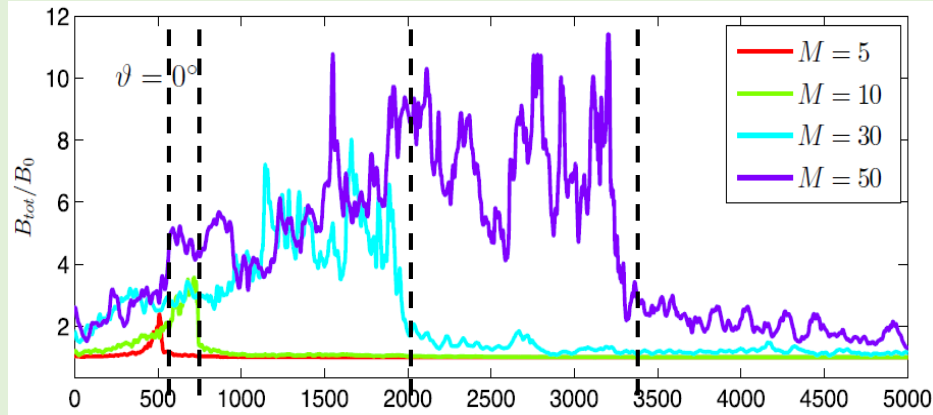
$M = 20$ shock



At parallel shocks
stream of accelerated ions
into upstream
→ self-generated waves
→ Turbulent B amplification

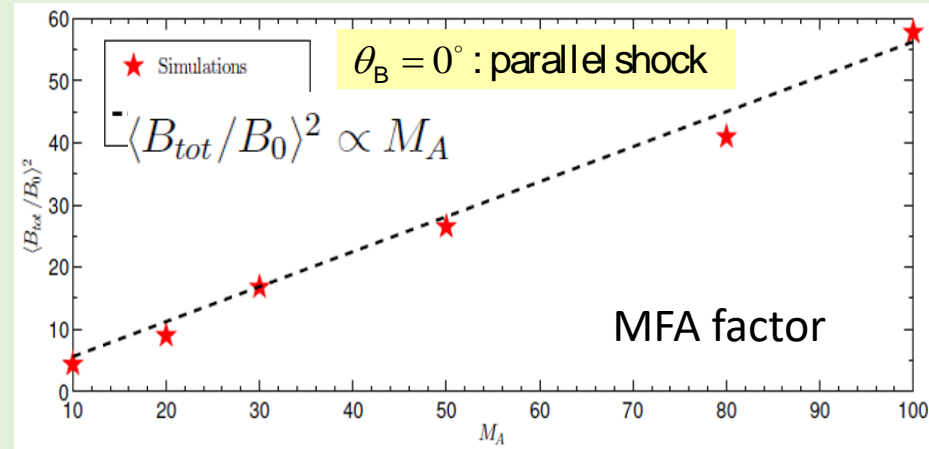
At Q-perp shocks
No accelerated ions into
upstream
→ No turbulent waves
→ No turbulent B field
amplification except
shock compression

Parallel shock

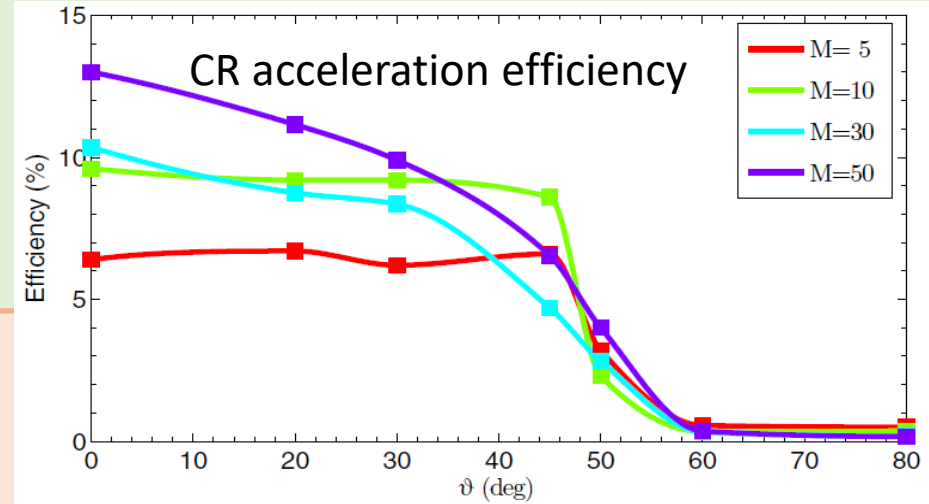
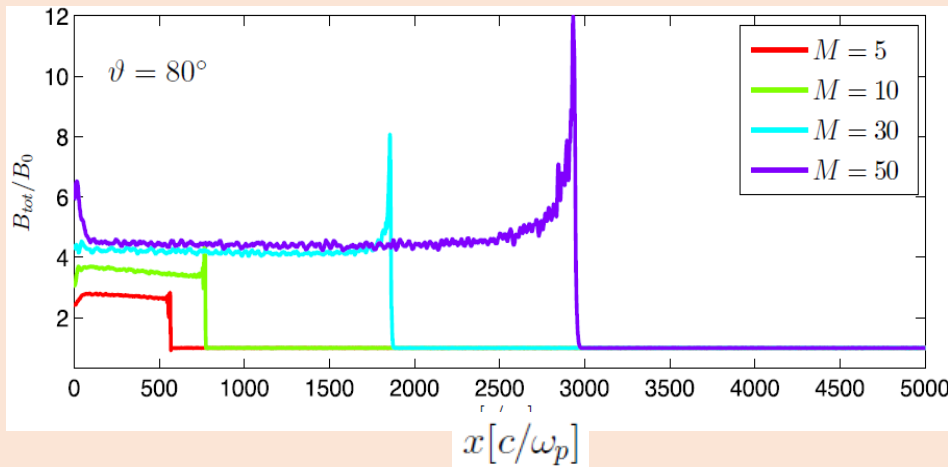


$x [c/\omega_p]$

Two stream instability
 \Rightarrow self-generated waves
 \Rightarrow amplification of B fields



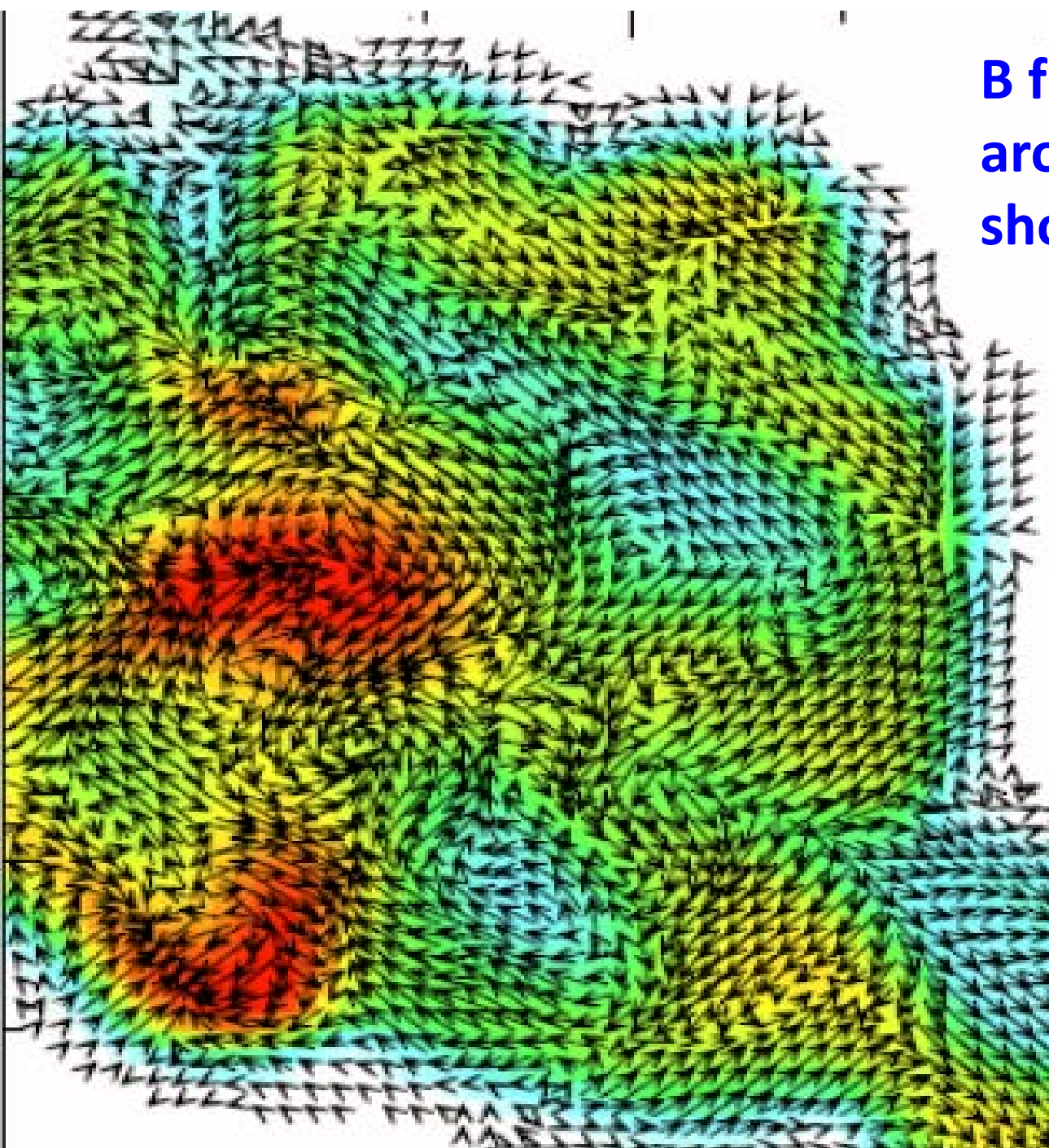
Quasi-perp shock



$B_2 = B_0 (\rho_2 / \rho_1)$
 only compression at the shock
 No self-generated waves
 No amplification

Caprioli & Spitkovsky 2014

**B field directions
around accretion
shocks: random**



Q-par shocks

Q-perp shocks

Cold Void Gas
 $T < 10^4$ K

$B \sim 1 - 10$ nG

$R_s \sim 3 - 5$ Mpc

$V_s \sim 10^3$ km/s

$B \sim 0.1$ μ G

B

B

Accretion shock

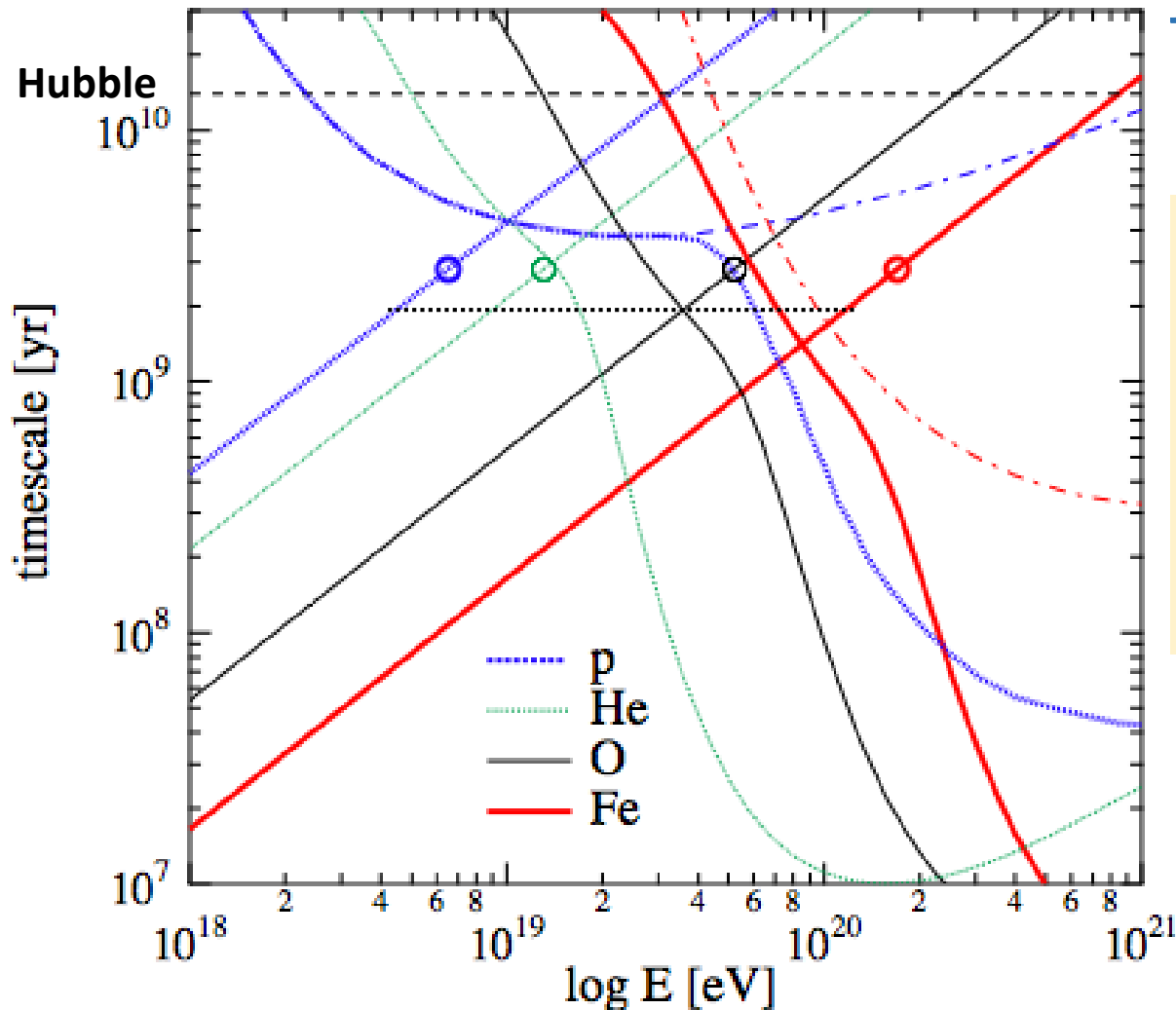
Hot shocked IGM
 $T > 10^6$ K

CR Nuclei from cluster accretion shocks

Inoue, Sigl, Miniati & Armengaud (ICRC2007)

$$\tau_{acc} \sim \tau_{pp} \Rightarrow E_{max}$$

acceleration vs CMB losses



$R_s \sim 3.2$ Mpc
 $V_s \sim 2200$ km/s
 $B_s \sim 1$ μ G

In the cluster outskirts

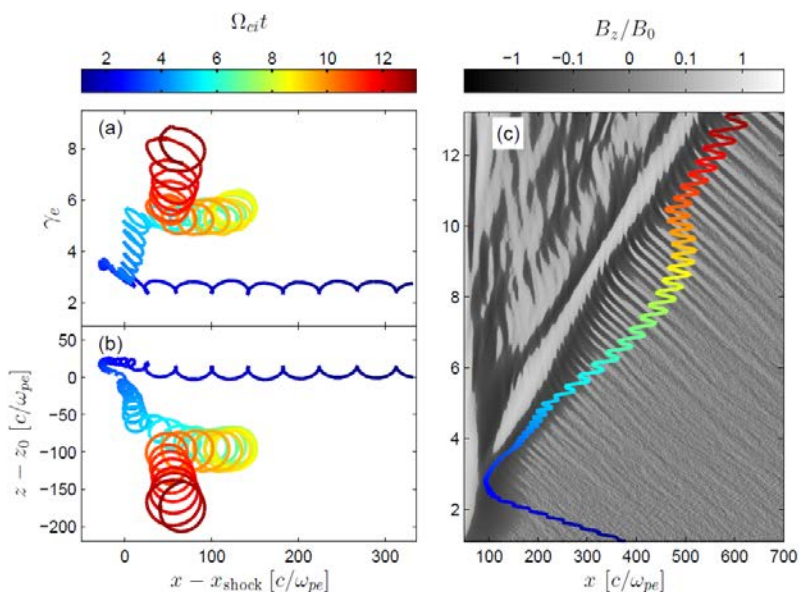
$B \sim 1 - 10$ nG

At Q-par shocks

$B_{shock} \sim 0.01 - 0.1$ μ G

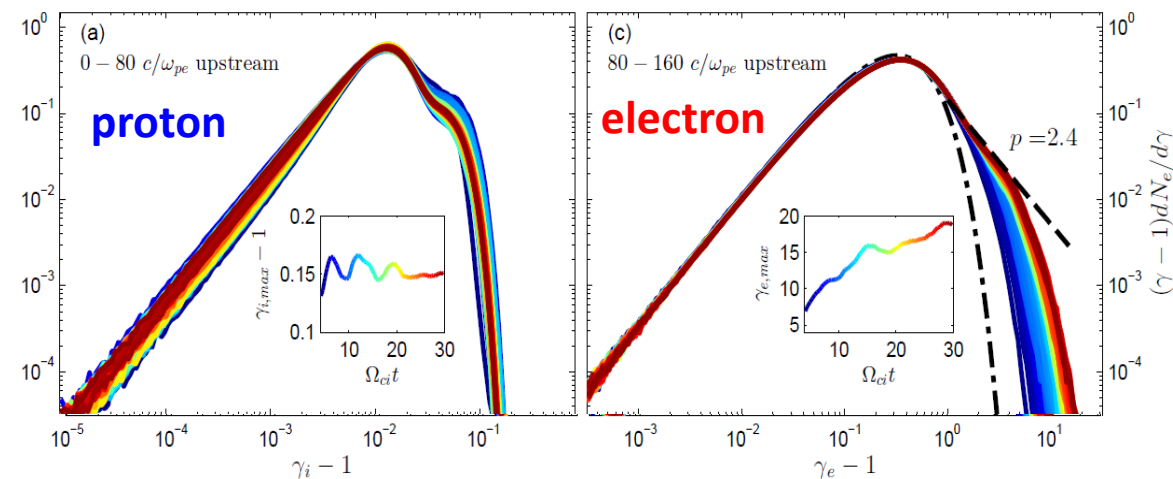
$\rightarrow E_{p, max} \sim 10^{18}$ eV

$\theta_{BN} = 63^\circ$, $M_A \approx 8.2$, $M_s = 3$, $u_0 = 0.15c$, $\beta_p \approx 25$: ICM shocks



Evolution of an electron undergoing multiple SDA

- Magnetic field compressed at the Q-perp shock
- ➔ Reflection of some electrons
- ➔ Induce temperature anisotropy in the upstream
- ➔ firehose instability excites waves
- ➔ Reflected electrons are scattered by the waves back to the shock downstream
- ➔ Undergo multiple SDA cycles



Minimal SDA for protons

➔ No acceleration

Multiple SDA for electrons

➔ suprathermal tail

➔ Pre-acceleration for DSA

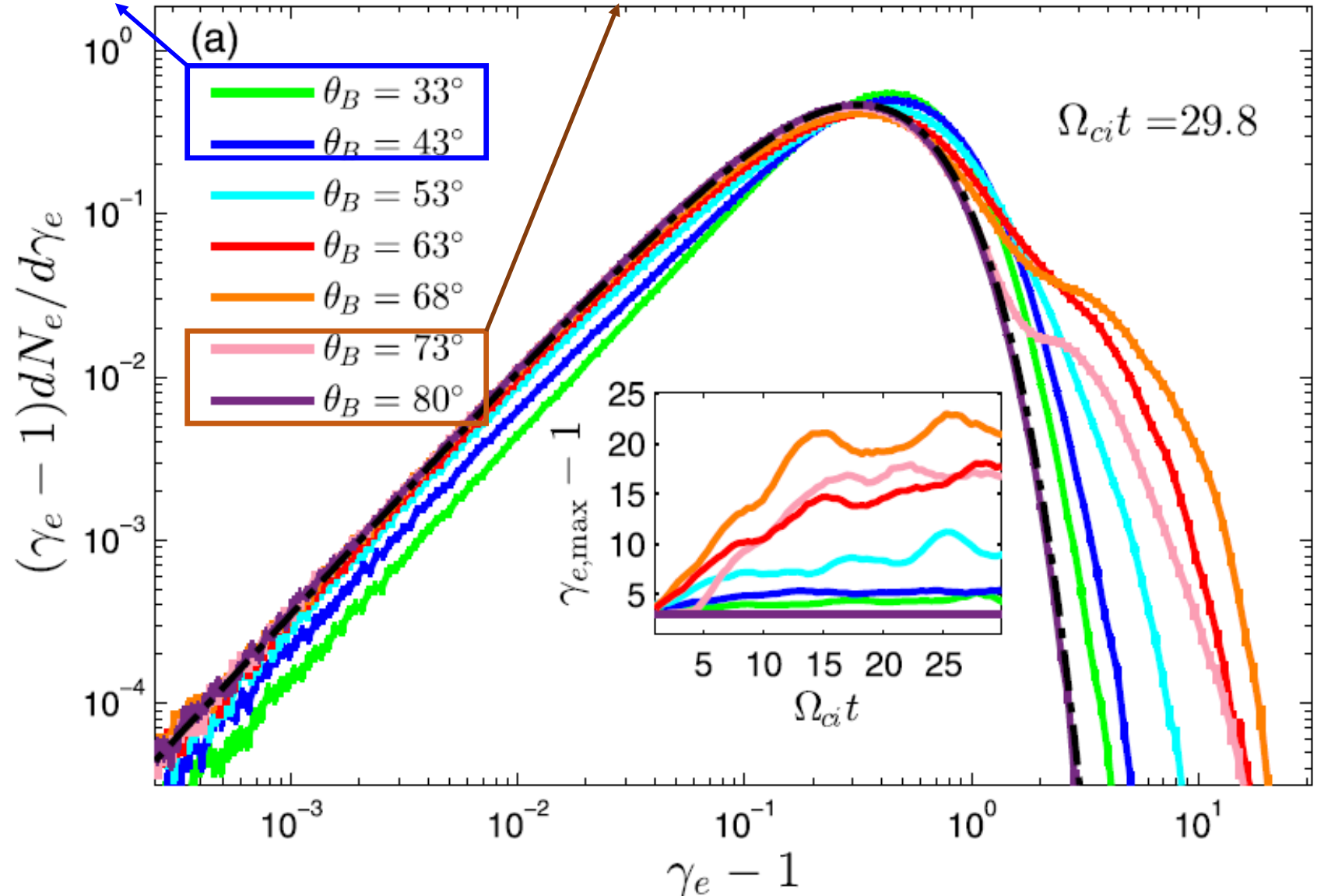
But Not yet full Fermi 1st order

DSA Obliquity Dependence: PIC Simulations (CRe)

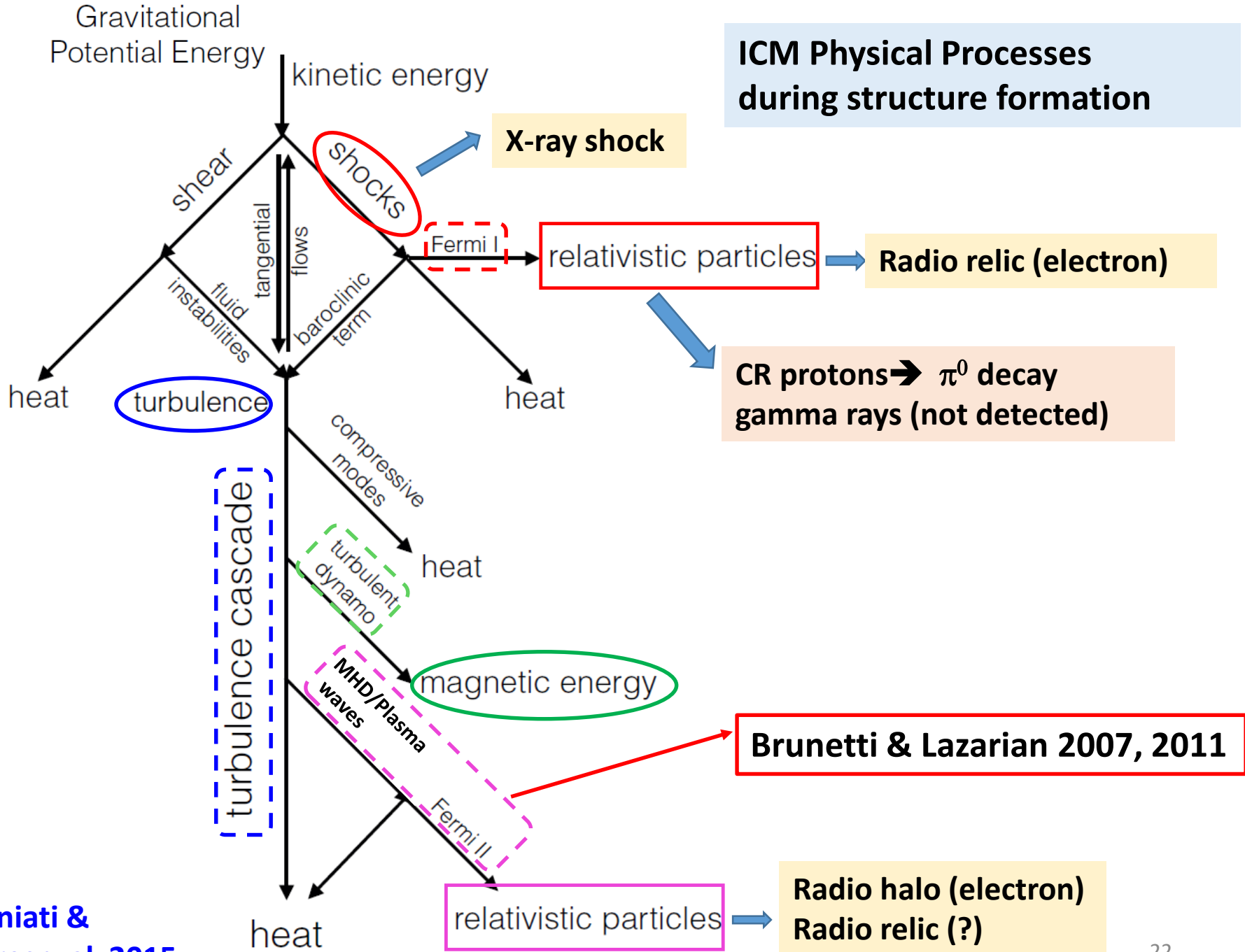
Guo, Sironi, & Narayan 2014

Slow acceleration of Fermi-I
at Q-par shocks

Inefficient reflection at
superluminal Perp shocks



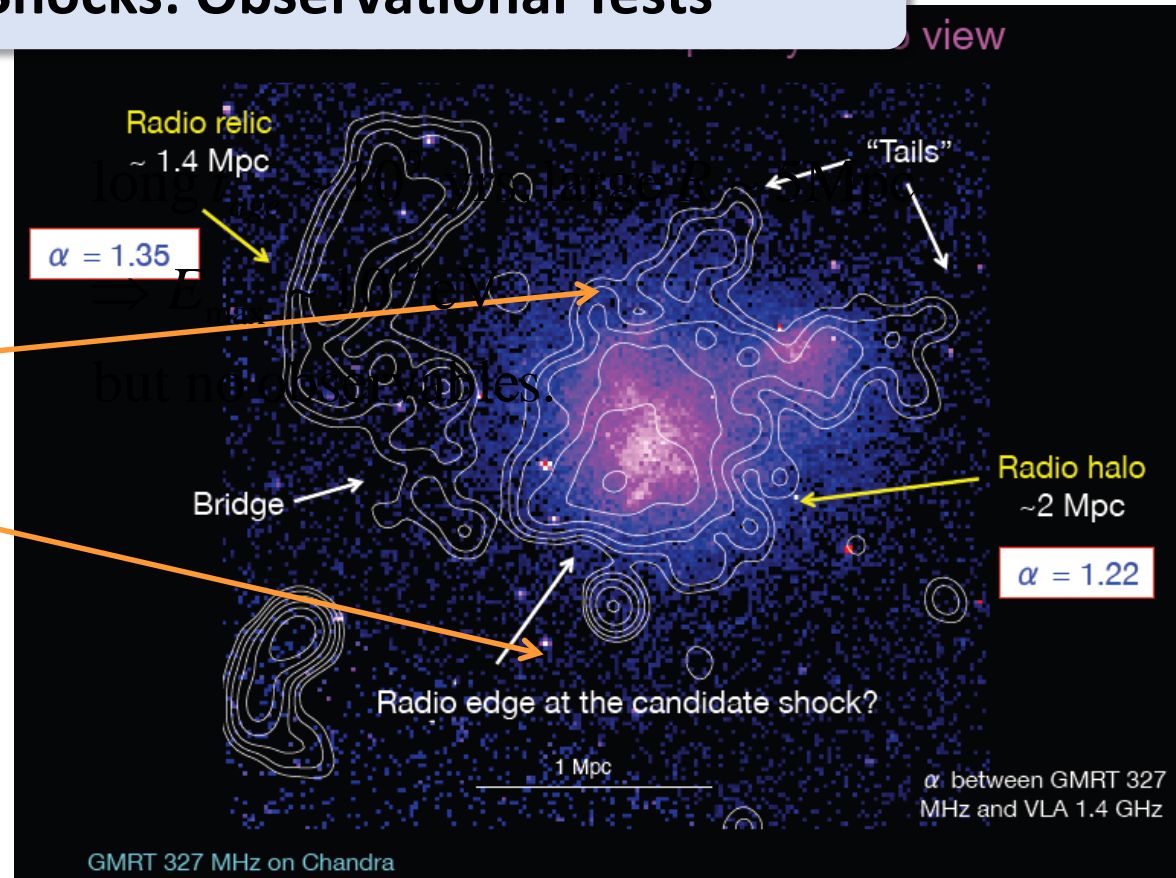
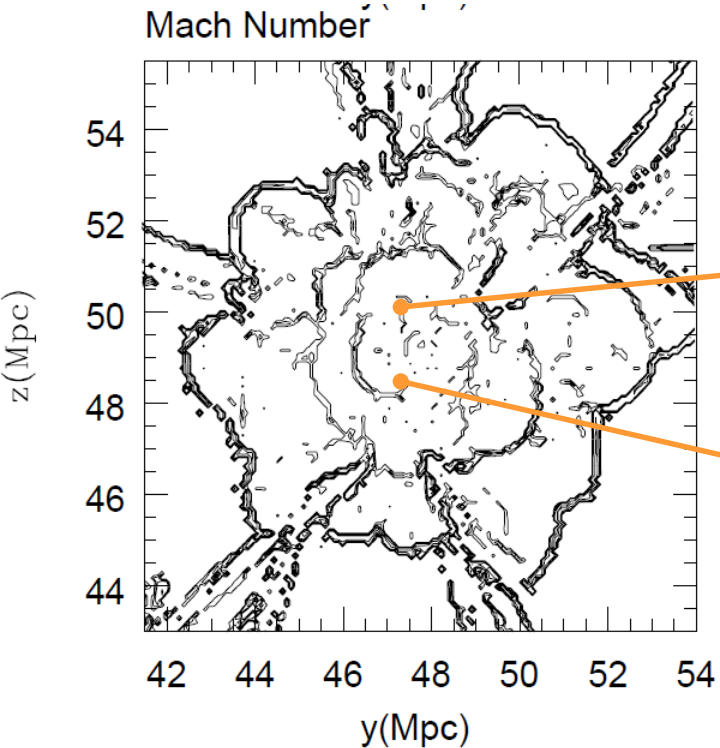
ICM Physical Processes during structure formation



Miniati & Beresnyak 2015

Brunetti & Lazarian 2007, 2011

Cosmological Shocks: Observational Tests



Shocks around clusters

X-ray halo hot ICM gas \rightarrow X-ray shocks

Radio halos: 2ndry electrons reaccelerated by turbulence (Brunetti +)

Radio relics: primary electrons (re)accelerated by shocks

Magnetic field: turbulent dynamo, shock amplification

γ -ray emission: π^0 decay (hadronic CRs) : **not detected**

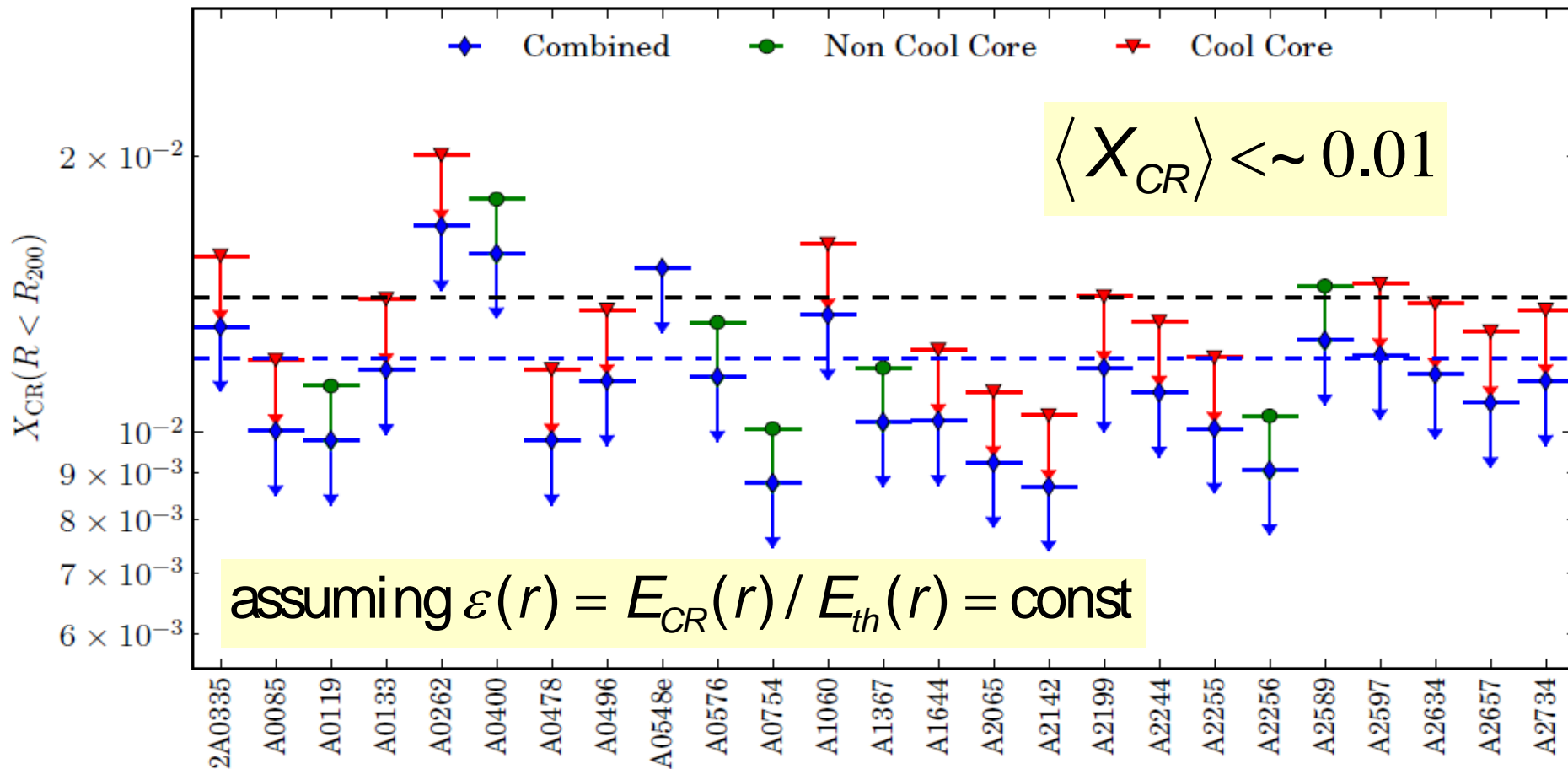
Accretion shocks: **not detectable**

Search for cosmic-ray induced γ -ray emission in Galaxy Clusters

The *Fermi*-LAT Collaboration:

Ackermann et al. 2013

the volume-averaged CR-to-thermal pressure $\langle X_{CR} \rangle$

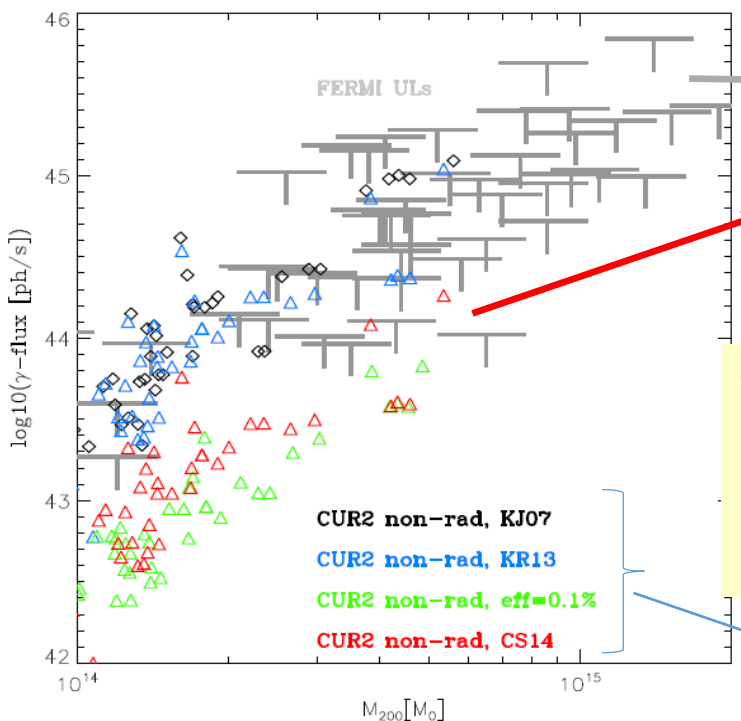
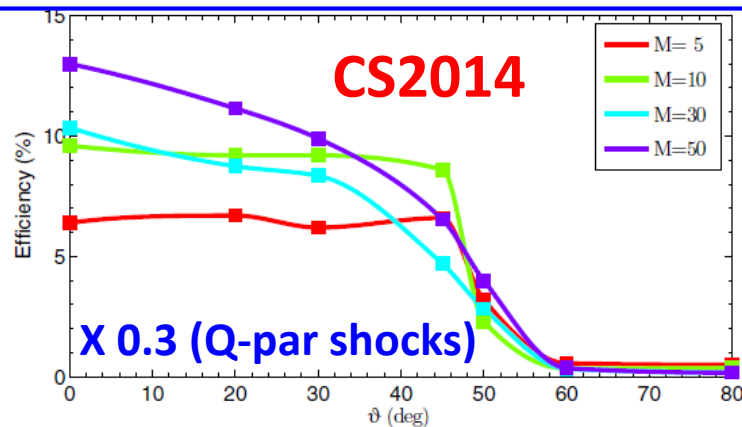
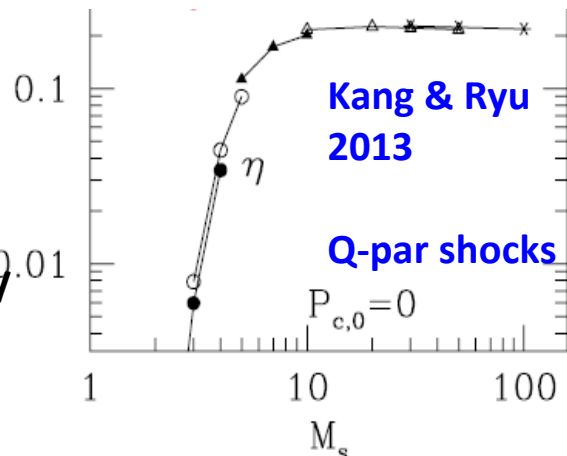


50 Galaxy Clusters in 4 years of Fermi LAT data

Constraining the efficiency of cosmic ray acceleration by cluster shocks

F. Vazza,¹★ M. Brüggen,¹ D. Wittor,¹ C. Gheller,² D. Eckert³ and M. Stubbe **2016**

Adopting CR proton acceleration efficiency based on DSA models, Estimate gamma-ray flux



Fermi LAT upper limits on gamma-ray flux from individual clusters

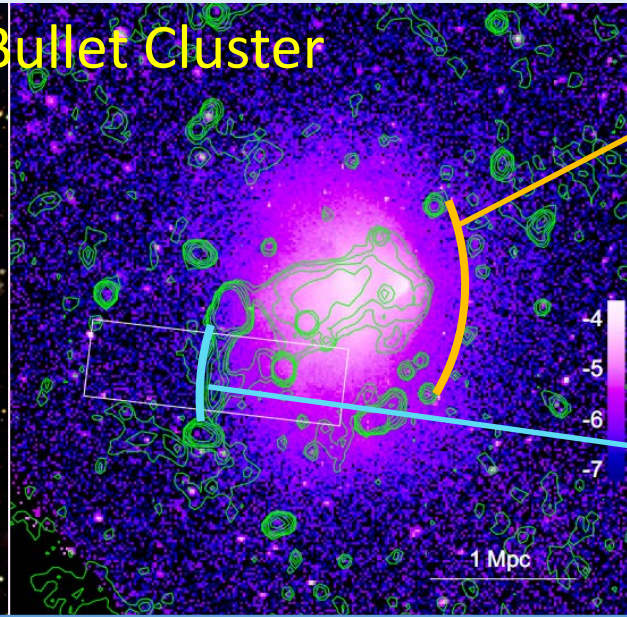
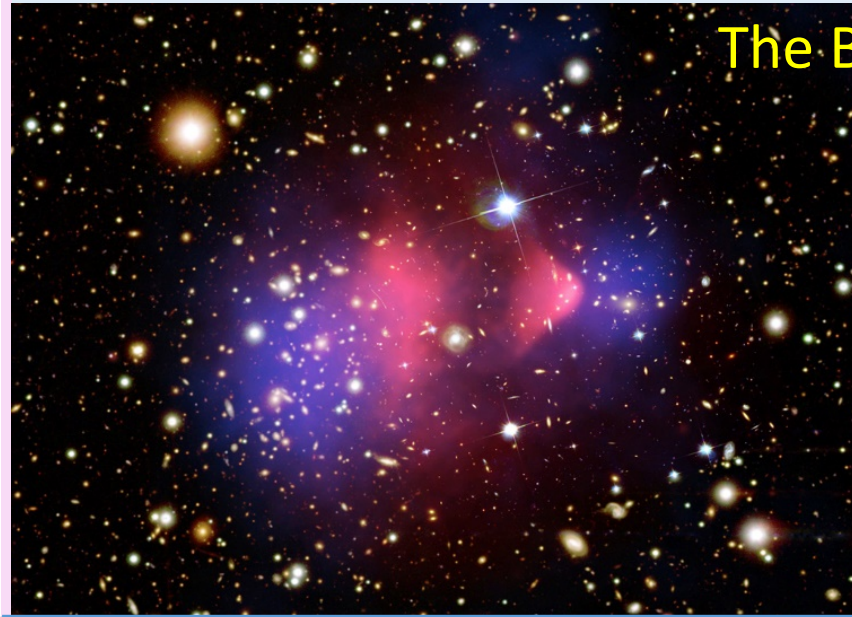
Gamma-ray flux of simulated clusters based on CS2014 DSA efficiency models

To be compatible with Fermi upper limits, the CR proton acceleration efficiency should be less than 10^{-3} for $2 < M < 5$ shocks.

Different DSA efficiency models

Signatures of shocks in ICM : X-ray observations

The Bullet Cluster

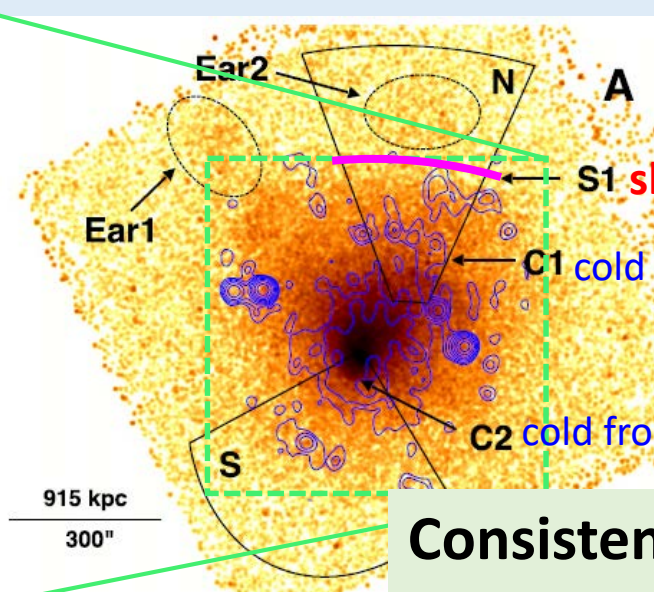
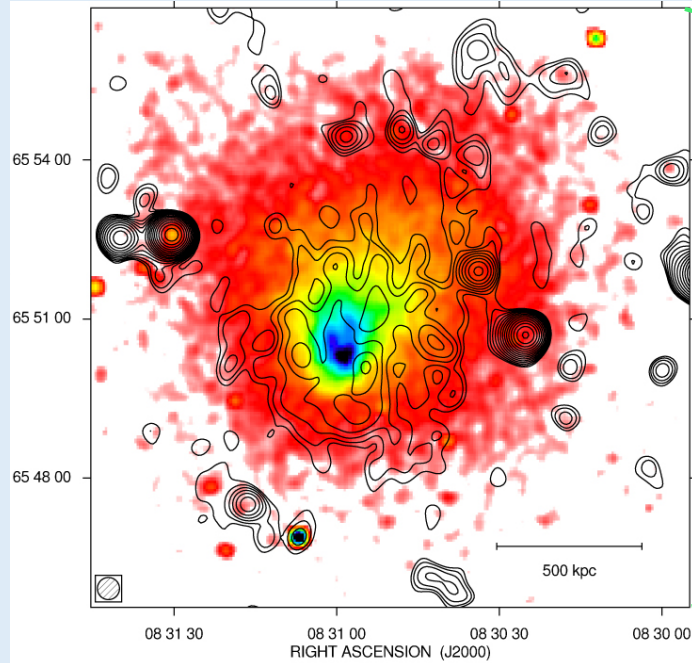


$M_X \approx 3.0$
(no associated radio relic)

Markevitch 2006

$M_X \approx 2.5$

Shimwell et al. 2015



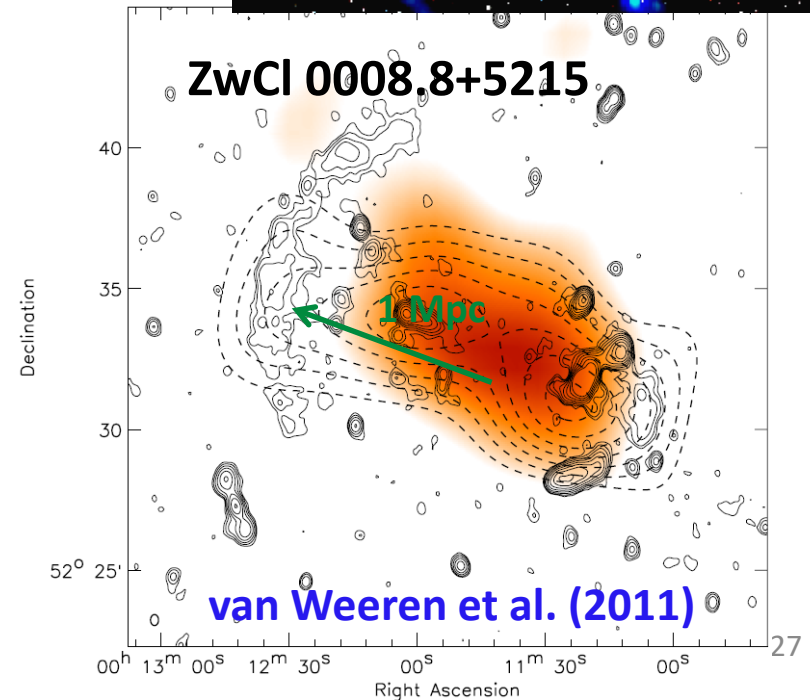
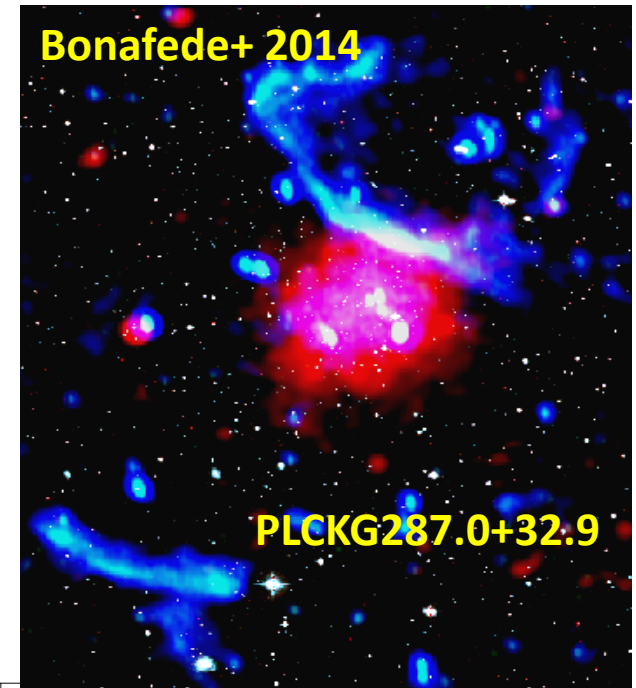
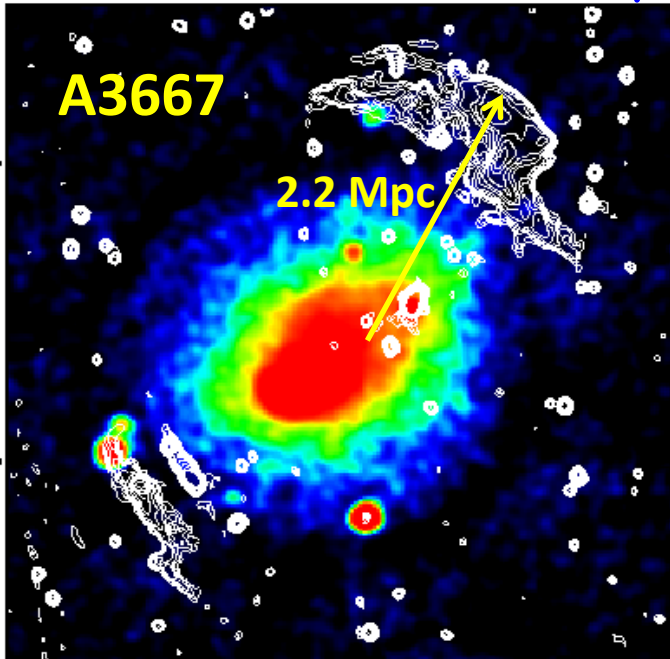
Cluster A665

$M_X = 3 \pm 0.6$
(no associated radio relic)

Dasadia et al. 2016

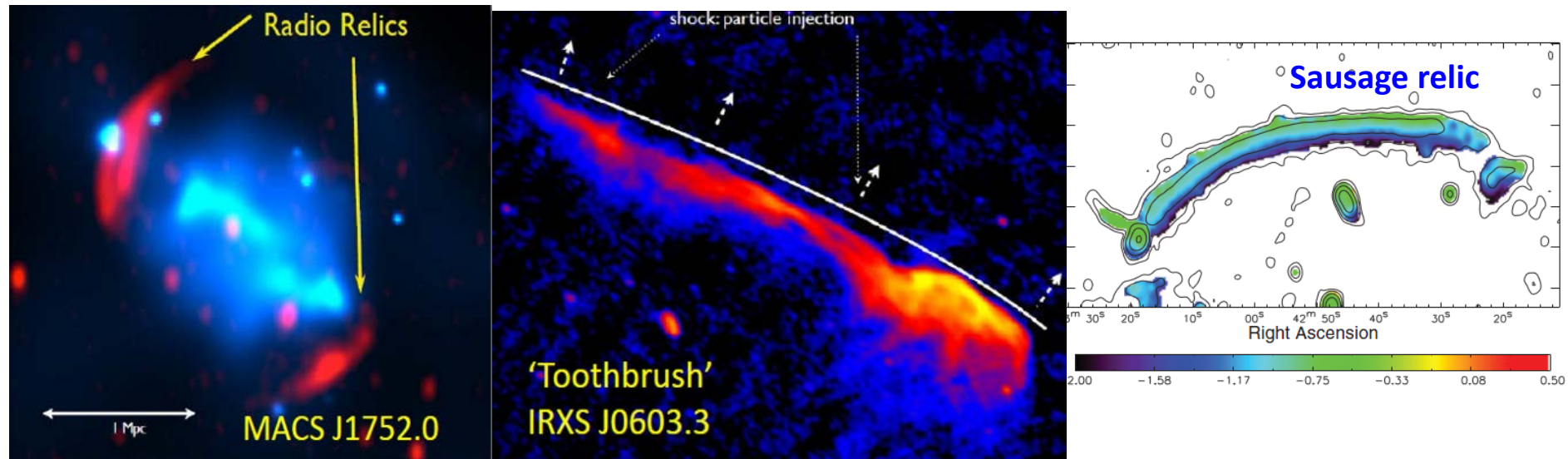
Consistent with theoretical predictions²⁶

~50 Radio Relics : diffuse synchrotron radiation from GeV electrons in μG B fields



Found in merging clusters.

Radio relics: diffuse radio sources found mainly in merging clusters

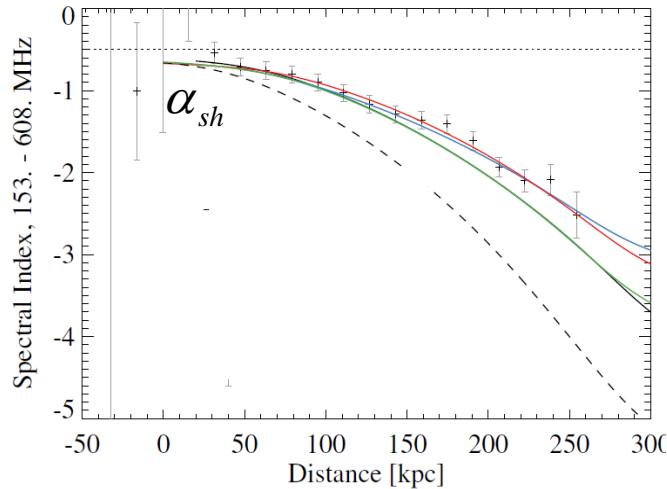


- elongated morphology
- spectral aging behind the shock (due to radiative cooling)
- power-law like integrated radio spectrum
- high polarization up to 50 % (B field compression across shock)

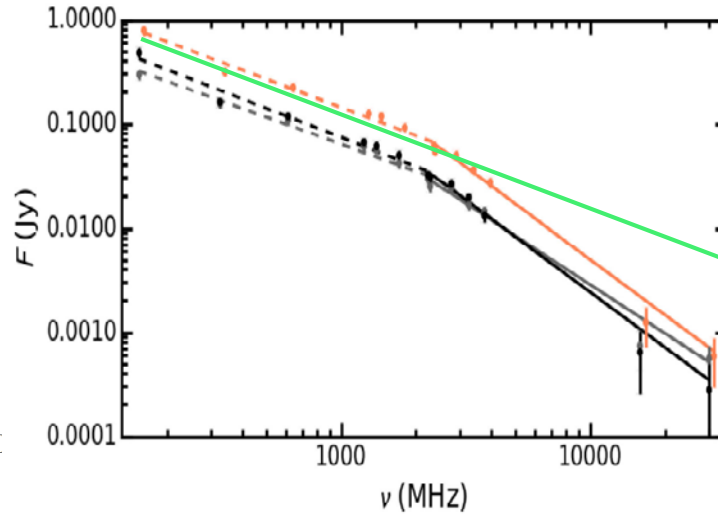
→ synchrotron radiation emitted by \sim GeV electrons accelerated at structure formation shocks

Radio vs. X-ray Observations of Radio Relics

Spectral index profile



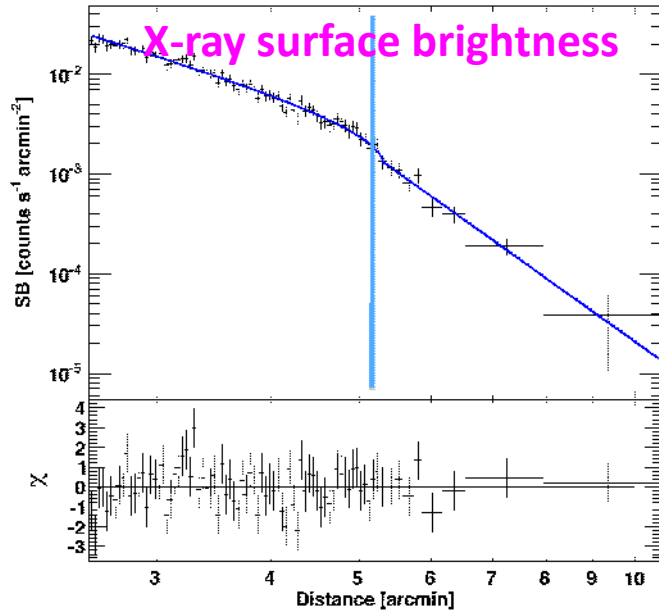
Integrated radio spectrum



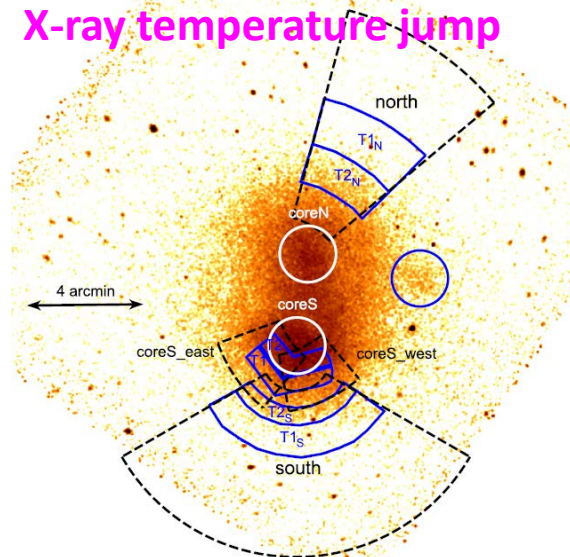
$$M_{radio}^2 = \frac{(3 + 2\alpha_{sh})}{(2\alpha_{sh} - 1)}$$

in situ injection model

$$\alpha_{integ} \approx \alpha_{sh} + 0.5$$



X-ray temperature jump

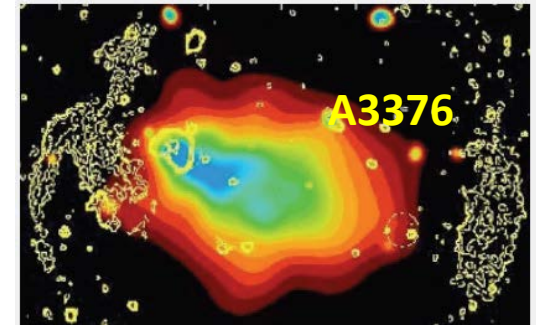
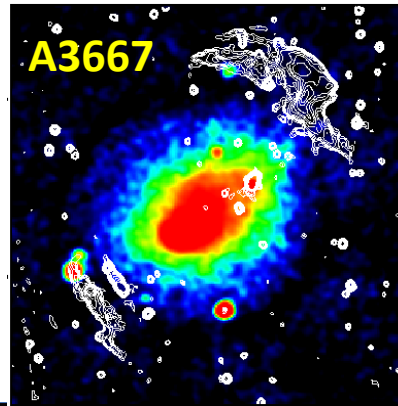
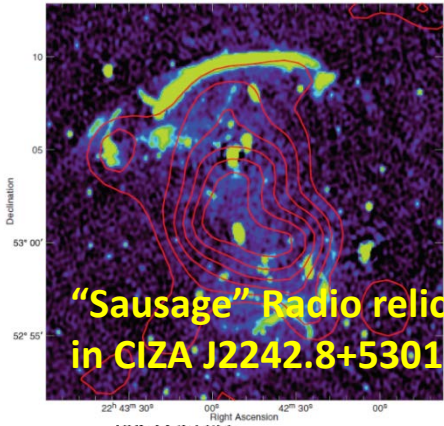


$$\frac{T_2}{T_1} = \frac{(M_X^2 + 3)(5M_X^2 - 1)}{16M_X^2}$$

$c_{s,1}$ = sound speed
 V_s = shock speed

* Projection effects

X-ray observations of radio relics: Akamatsu & Kawahara 2013



(b)A3376

(c)A3667

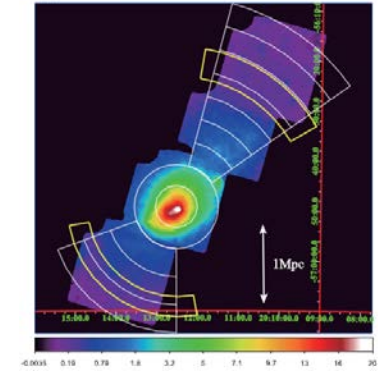
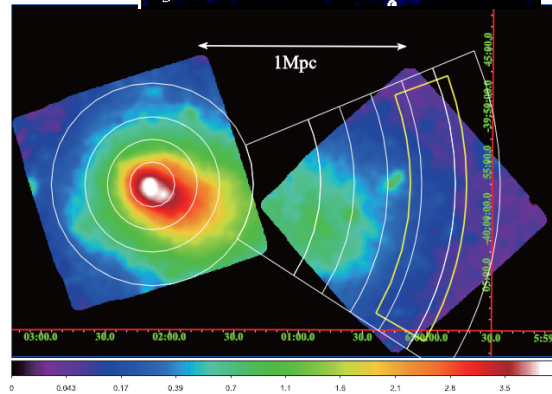
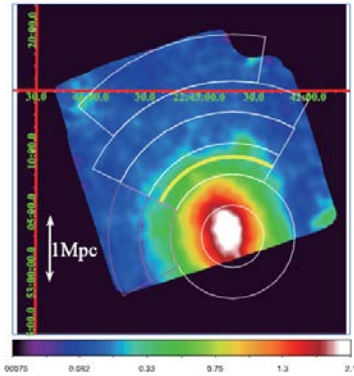
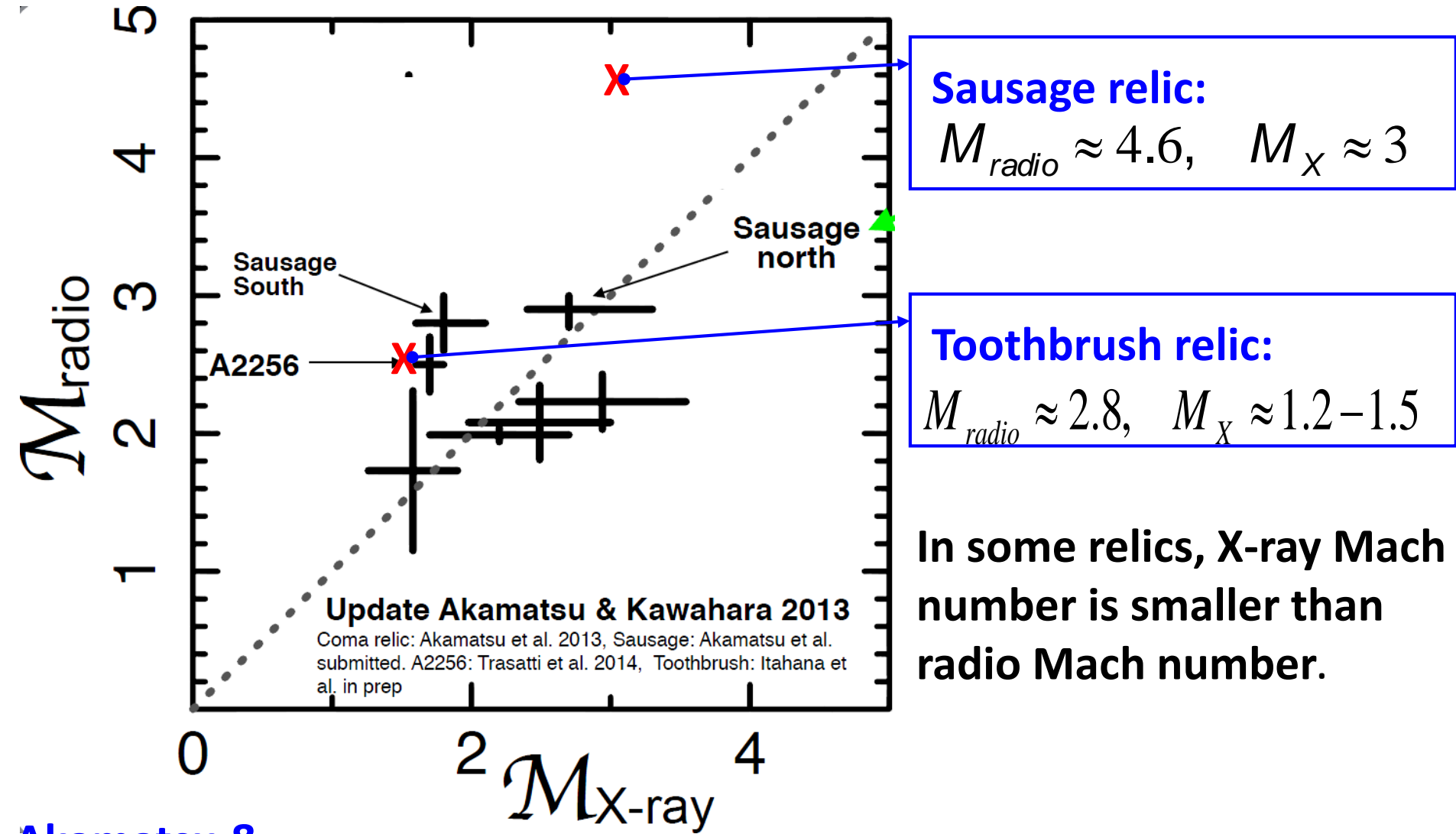


Table 4. Post- and pre-shock ICM quantities and Mach number derived from X-ray and radio observations.

	$kT_{\text{post shock}}$ (keV)	$kT_{\text{pre shock}}$ (keV)	$M_{X,kT}$	α	M_{radio}
CIZA2242	$8.33 \pm 0.80 \pm 0.40^*$	$2.11 \pm 0.44^{+2.10}_{-0.20}^*$	$3.15 \pm 0.52^{+0.40}_{-1.20}^*$	-0.60 ± 0.05	4.58 ± 1.32
A 3376	4.81 ± 0.29	1.35 ± 0.35	2.94 ± 0.60	-1.00 ± 0.10	2.23 ± 0.20
A 3667 NW	5.52 ± 0.95	2.03 ± 0.34	2.41 ± 0.39	-1.10 ± 0.20	2.08 ± 0.37
A 3667 SE	6.34 ± 0.38	3.59 ± 0.28	1.75 ± 0.13	-1.50 ± 0.17	1.73 ± 0.58

Mach numbers from X-ray and Radio observations of Radio Relics



Sausage relic:

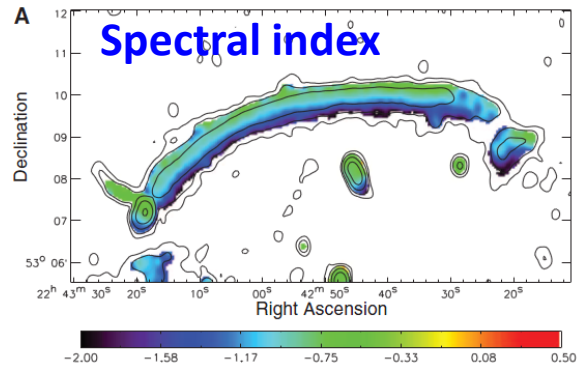
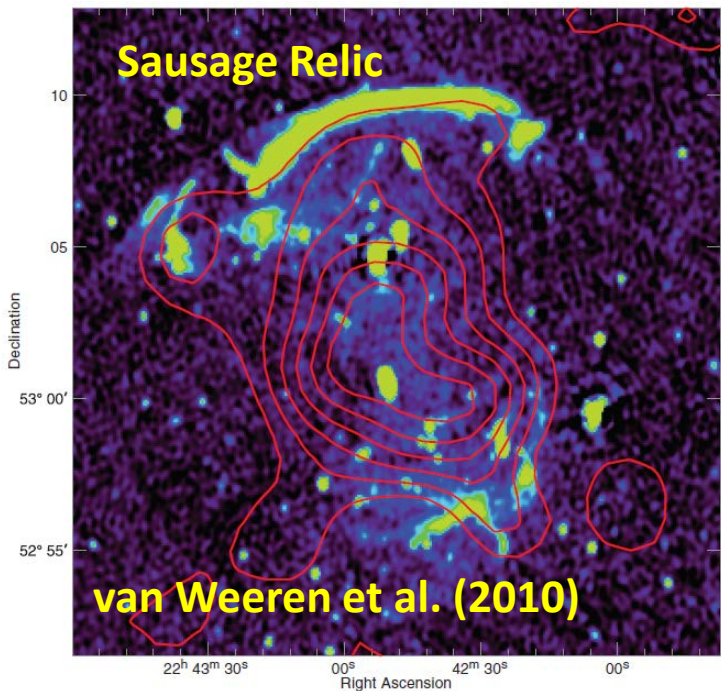
$$M_{radio} \approx 4.6, \quad M_X \approx 3$$

Toothbrush relic:

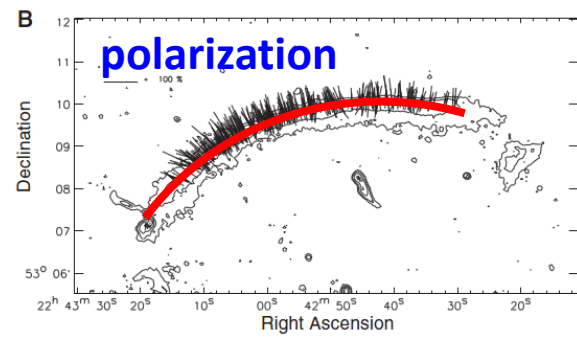
$$M_{radio} \approx 2.8, \quad M_X \approx 1.2-1.5$$

In some relics, X-ray Mach number is smaller than radio Mach number.

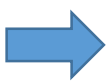
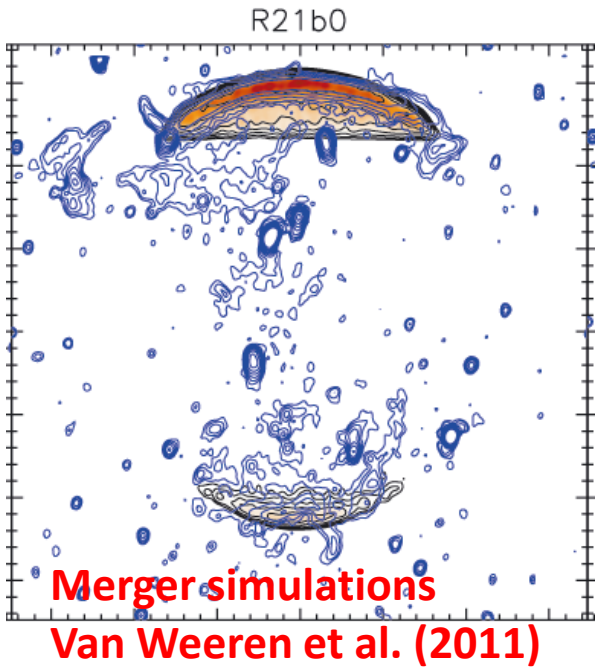
**Akamatsu &
Kawahara 2013**



Radiative cooling behind the shock



B line along the relic
 → Quasi-perp. shock



If the shock is a part of a spherical surface and if CR e are injected/accelerated at shocks.

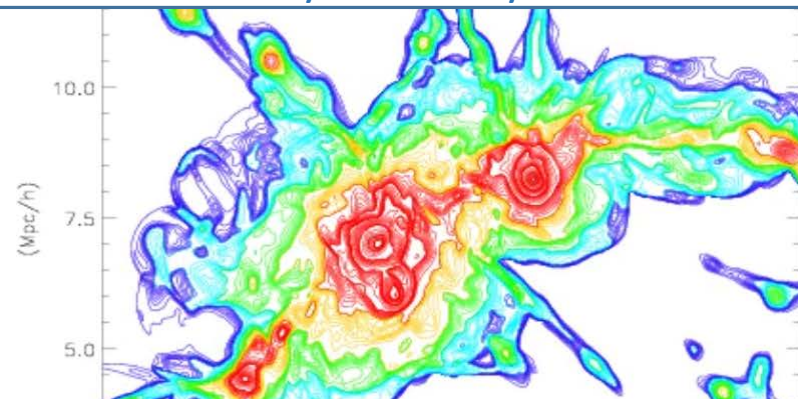
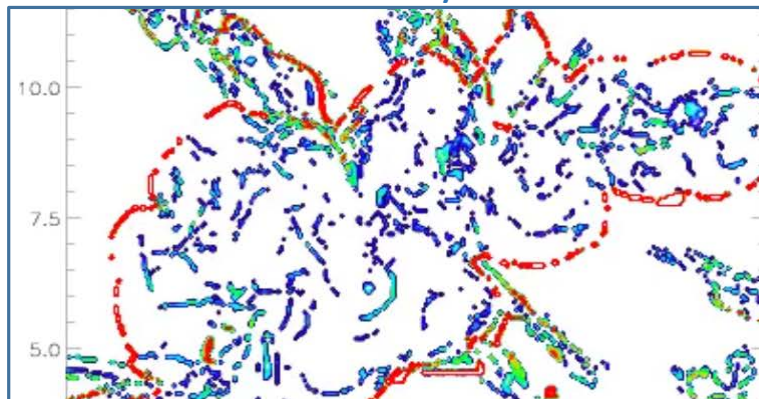
Q: Why are surface brightness and spectral index are uniform along the relic ?

Ubiquitous presence of structure formation shocks in ICM

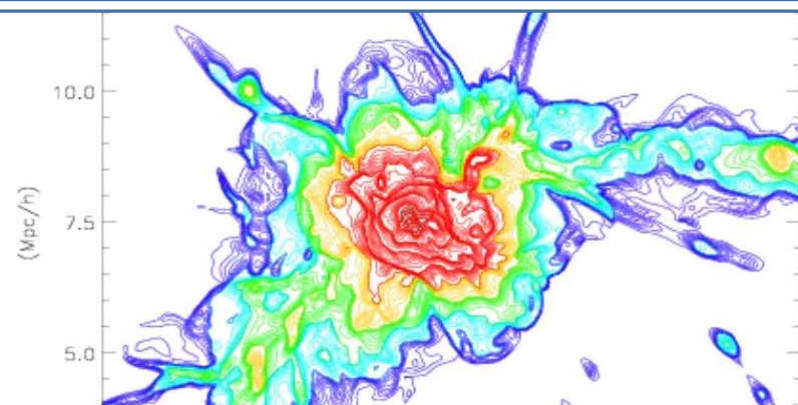
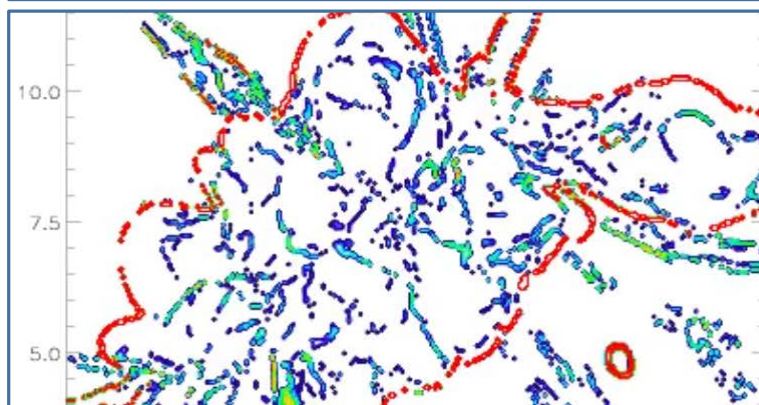
Shock distribution by Mach number

X-ray emissivity

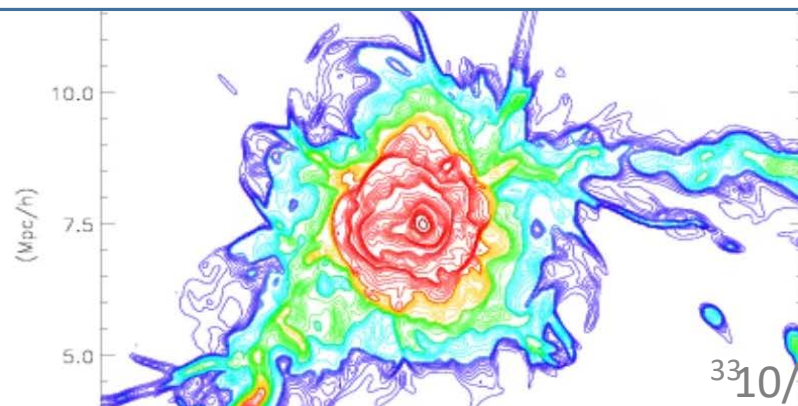
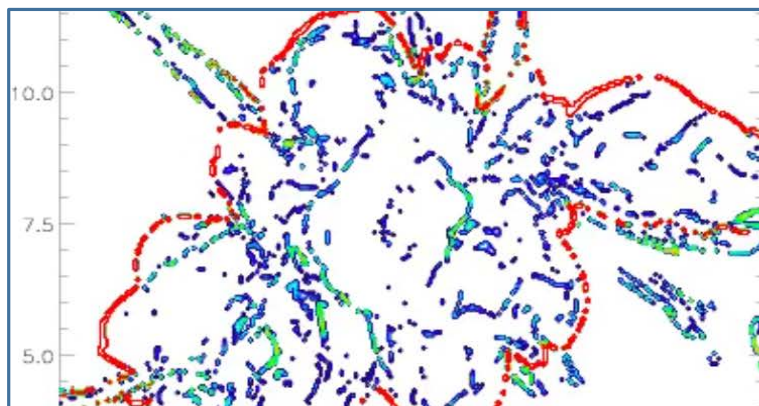
Z=0.65



Z=0.30



Z=0.22



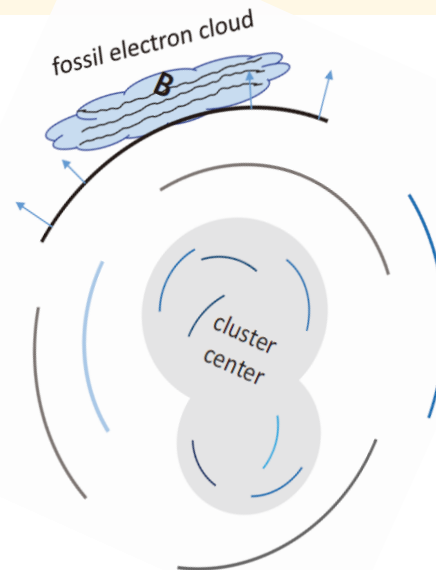
Ha, Ryu,
& Kang
2016

Puzzles for *in situ* injection model

- (1) Why for some radio relics, $M_{radio} > M_X$
- (2) Low *in situ* injection and acceleration efficiency at weak shocks ($M < 3$)
- (3) Why only ~10 % of merging clusters host radio relics, while numerous shocks are expected to form in ICM ?
- (4) Why some X-ray shocks do not have associated radio relics ?

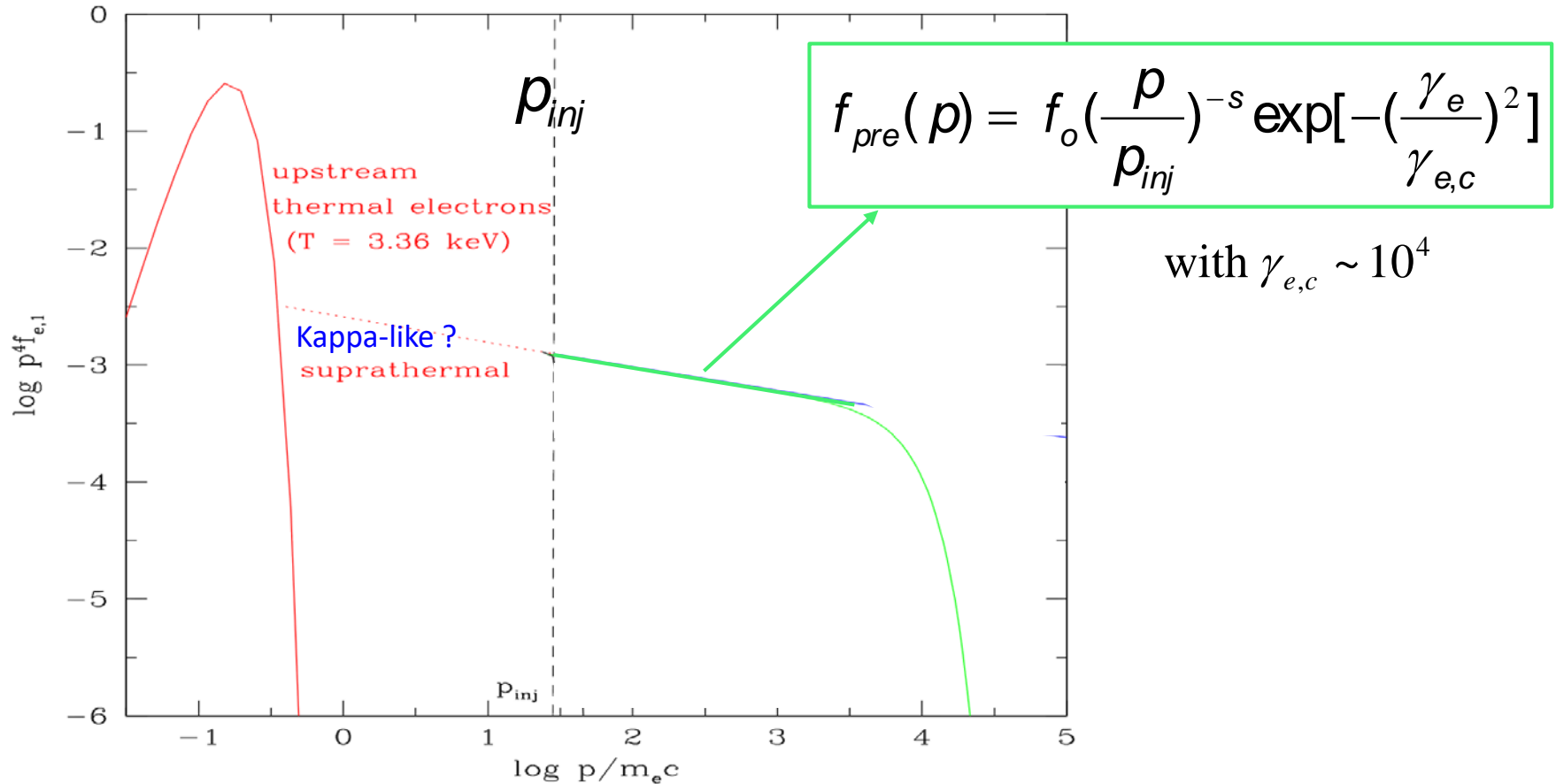
Reacceleration model can solve these puzzles:

a radio relic forms when a weak shock encounters the ICM plasma with **pre-existing** electrons.



Kang & Ryu (2015)

Solution: Re-acceleration of Pre-existing electrons



radio spectral index α is determined by M_s , s , & $\gamma_{e,c}$

$\Rightarrow M_{radio} \neq M_s$ or M_x (not necessarily)

Puzzles for *in situ* injection model

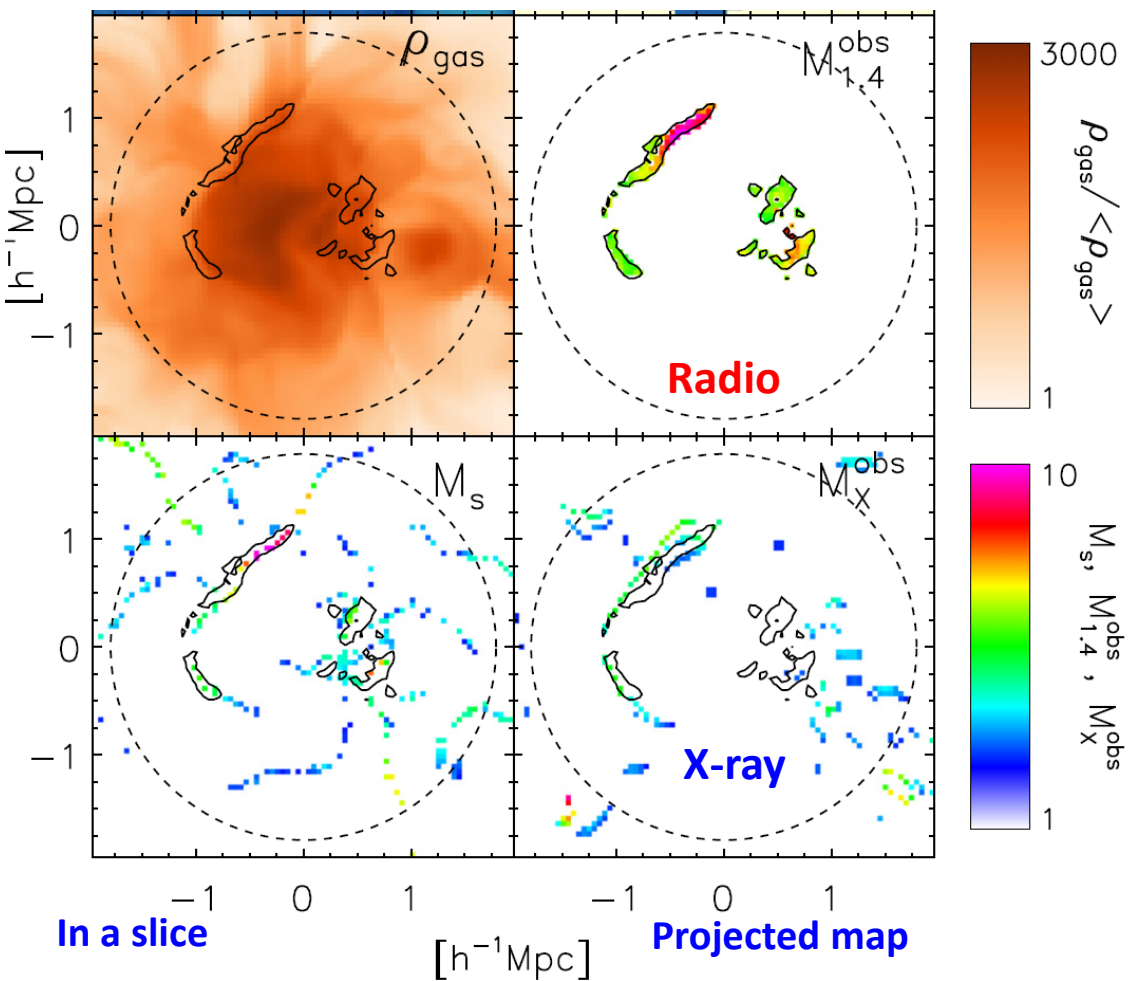
- (1) Why for some radio relics, $M_{radio} > M_X$
- (2) Low *in situ* injection and acceleration efficiency at weak shocks ($M < 3$)
- (3) Why only ~10 % of merging clusters host radio relics, while numerous shocks are expected to form in ICM ?
- (4) Why some X-ray shocks do not have associated radio relics ?

Reacceleration model can solve these puzzles:

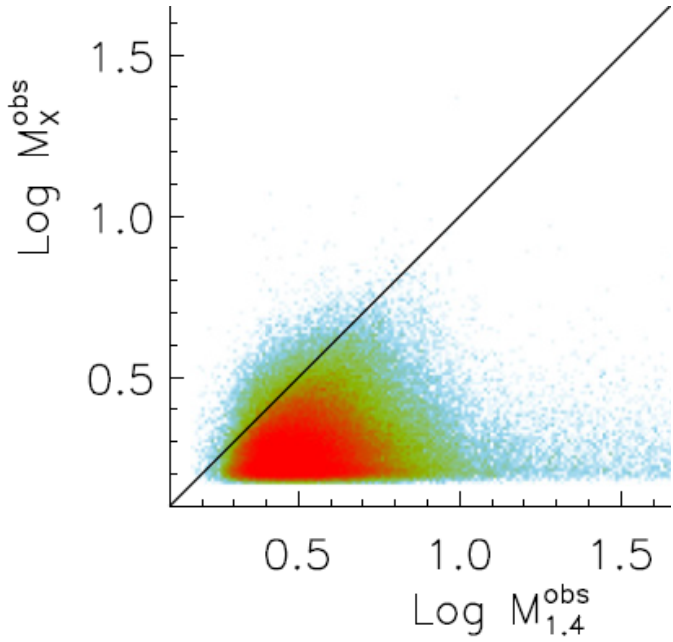
a radio relic forms when a weak shock encounters the ICM plasma with **pre-existing** electrons.

- (1) radio spectral index α is determined by M_s , s , & $\gamma_{e,c}$
 $\Rightarrow M_{radio} \neq M_s$ or M_X (not necessarily)
- (2) fossil electrons \Rightarrow seed electrons to DSA
- (3)(4) Not all shocks can accelerate electrons and become radio relics.

Mock observation of X-ray vs. Radio Shocks in the simulated clusters



Radio vs. X-ray Shock Mach no.



$M_X^{\text{obs}} < M_{\text{radio}}^{\text{obs}} \sim M_s$
 due to projection effects &
 lack of spatial resolution

Contour: 1.4 GHz radio flux

$M_{1.4}^{\text{obs}}$: derived from spectral index btw 140MHz and 1.4GHz

M_X^{obs} : derived from T_X jump across the shock

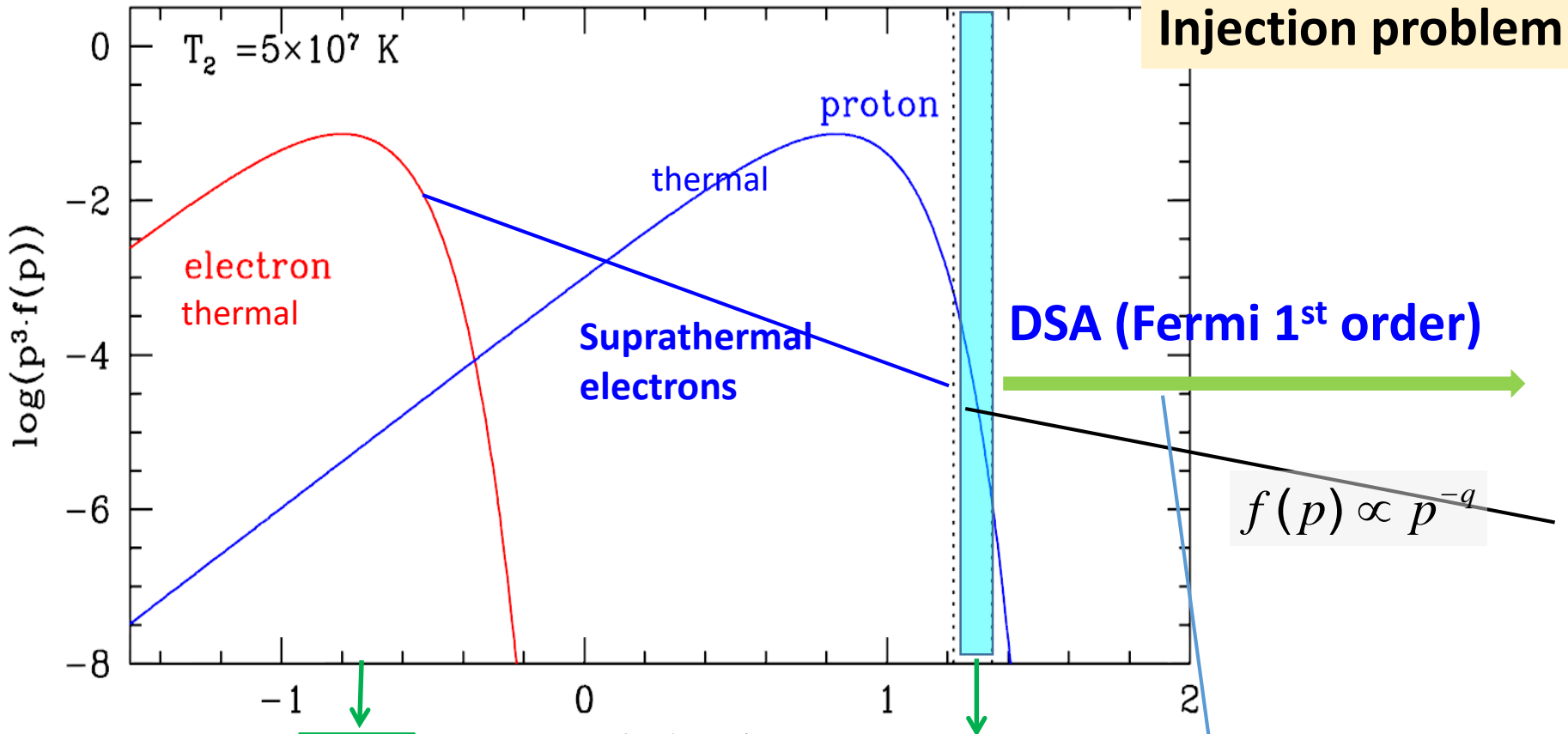
M_s : true shock Mach number

Going beyond the Standard Models ?

Need to go deeper into the Standard Models !

**In particular, we need to understand Collisionless Shocks with low Mach numbers in high beta plasma.
e.g. Injection Problem is not a DSA problem.
It is a problem of plasma kinetic processes.**

Injection problem



$P_{th,e}$ **electron injection**

$$p_{inj} \sim 3\sqrt{2m_p k_B T_2} \sim 130 p_{th,e}$$

$$\lambda_{mpf} \geq 3r_g(p_{th,p}) \sim \text{shock thickness}$$

Plasma Kinetic processes:
 wave-particle interactions
 pre-heating due to instabilities
 PIC/Hybrid simulations

MHD waves
 Fokker-Planck Equation
 DC equation

Summary

1. Shocks are abundant in and around galaxy clusters:

- external accretion shocks: $10 < M < 10^2$: **not detected (not detectable)**
- internal shocks driven by mergers and chaotic flow: $M < 3$ } **Radio relics**
- infall shocks induced by infalls along filaments: $3 < M < 10$ } **X-ray shocks**

2. Mean IGMF is 0.1-1 μ G in ICM, while 1-10 nG in filaments and cluster outskirts

3. Cluster accretion shock may accelerate protons up to 10^{18} eV.

4. CR/Gas energy ratio in ICM constrained by γ -ray observations: $\langle X_{CR} \rangle < \sim 0.01$

5. Mock observations of simulated clusters in the projected maps:

→ $M_{X\text{-ray}} \leq M_{\text{radio}}$ due to projection effects

6. Re-acceleration model can explain most of observed features of radio relics

7. DSA efficiency & MFA at shocks with $2 < M < 5$ in high beta plasma need

to be studied with plasma simulations: $\eta(M, \theta)$, B/B_0

Review Papers: Bruggen et al. 2012, Brunetti & Jones 2014, 2015, Ryu et al. 2012